

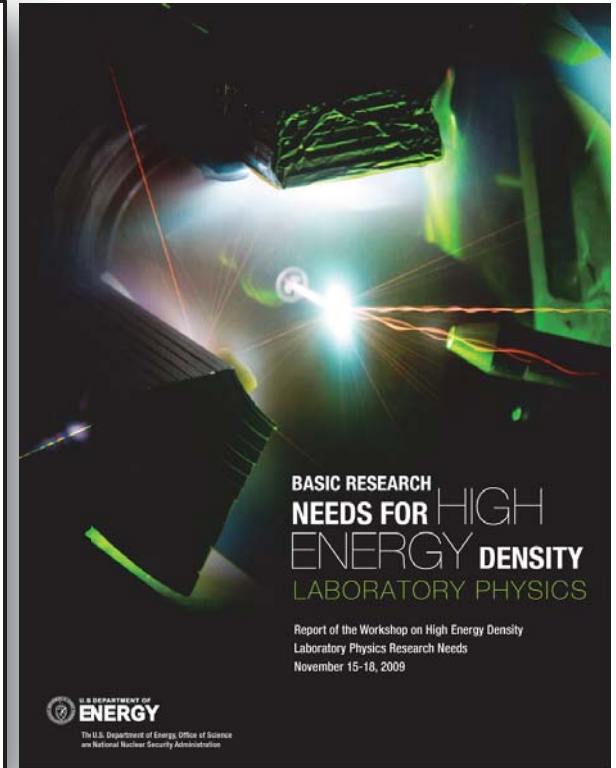
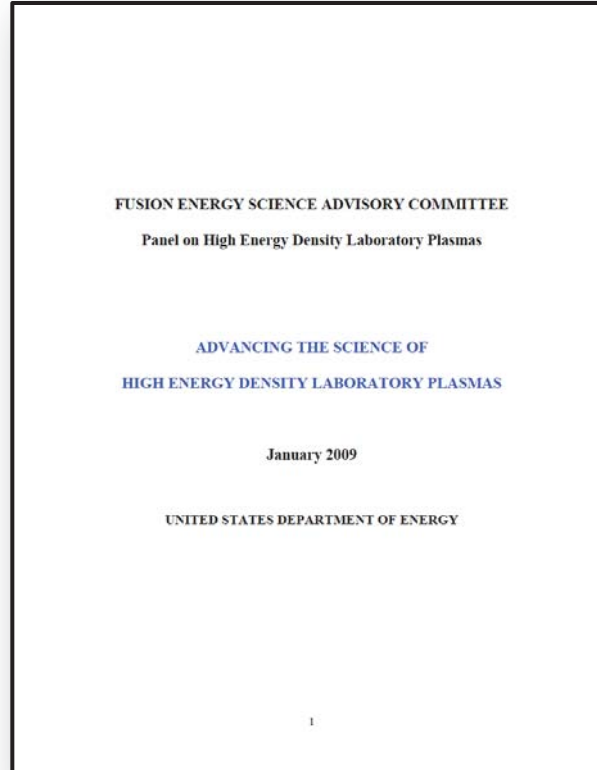
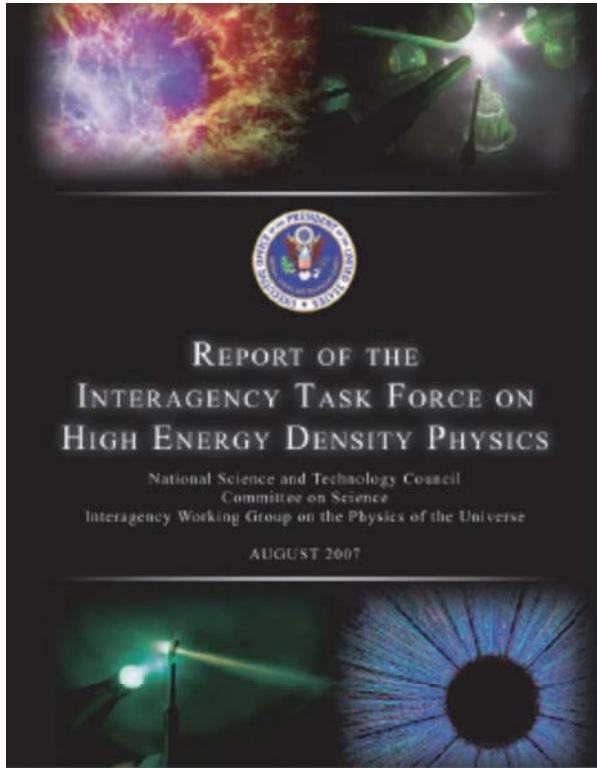
# The Jupiter Laser Facility – An Update



**Robert Cauble**  
**JLF Director**  
**NIF/JLF User Group Meeting**

**February 11-13, 2013**

# DOE-sponsored reports have made recommendations for research in HED science



**The reports all call for teaching HED science, broadening HED research, strengthening academic ties to DOE laboratories, and giving the broader community access to HED experimental facilities**

Access to facilities?

# What facilities?

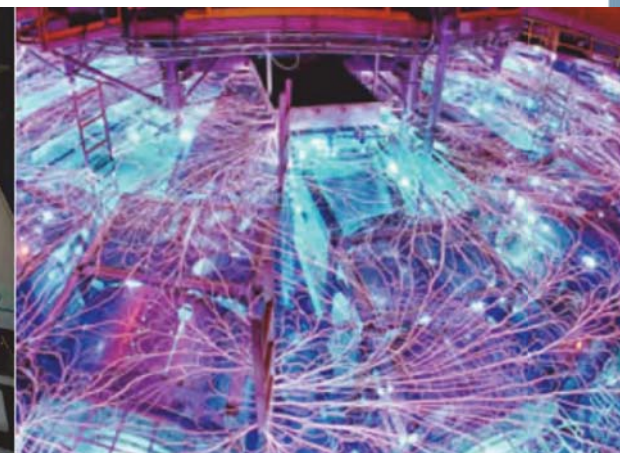
**Large lasers**



**Not-quite-so-large lasers**



**Large pulsed power devices**



**National Ignition Facility  
LLNL**

**Texas Petawatt  
UT - Austin**

**Z Machine  
Sandia Nat Lab**

It is generally very hard to get to use places like these



# Jupiter Laser Facility



Expanding High Energy-Density Science

# Jupiter is a multi-platform intermediate-scale facility for high energy-density (HED) science



## Mission

- Expand the frontiers of high energy-density laboratory science
- Support high energy-density science at LLNL in multiple programs
- Support, collaborate with, and expand the broader HED physics community
- Help train and recruit future scientific workforce

## Approach

- Office-of-Science-style user facility at which laser time is provided free-of charge and apportioned through an open, competitive peer-review process
- On a scale that provides significantly more laboratory access and greater flexibility than large-scale laser facilities
- With a variety of platforms capable of front-rank HED science for different classes of experiments
- And the infrastructure to safely support multiple users with a range of experience levels

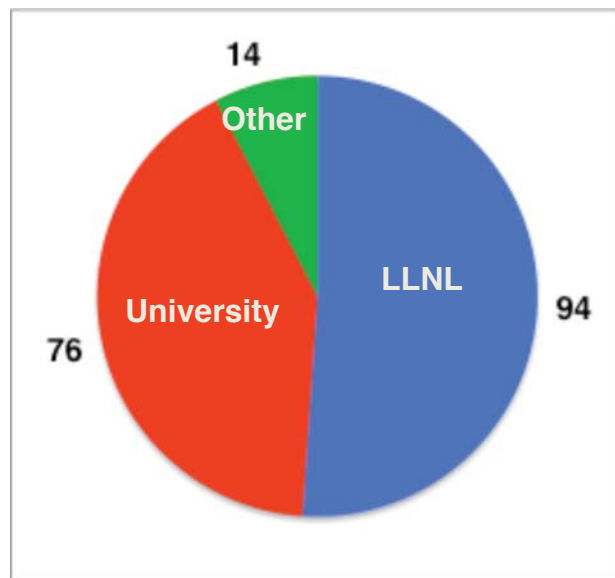


as well as in Europe and Asia



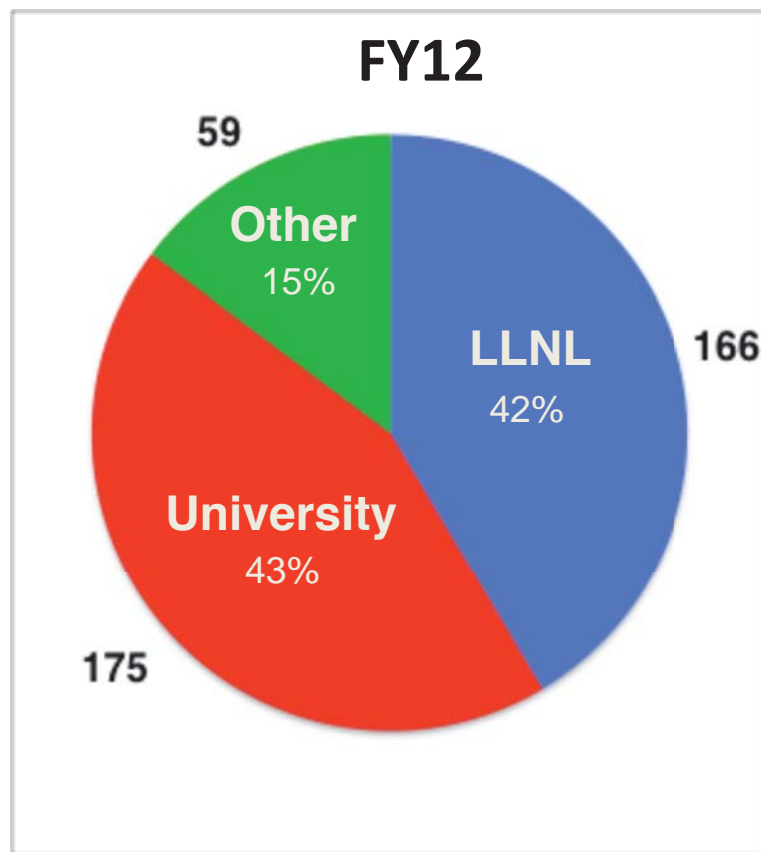
# Number of active JLF users continues to increase

In 2008 JLF had 184 users



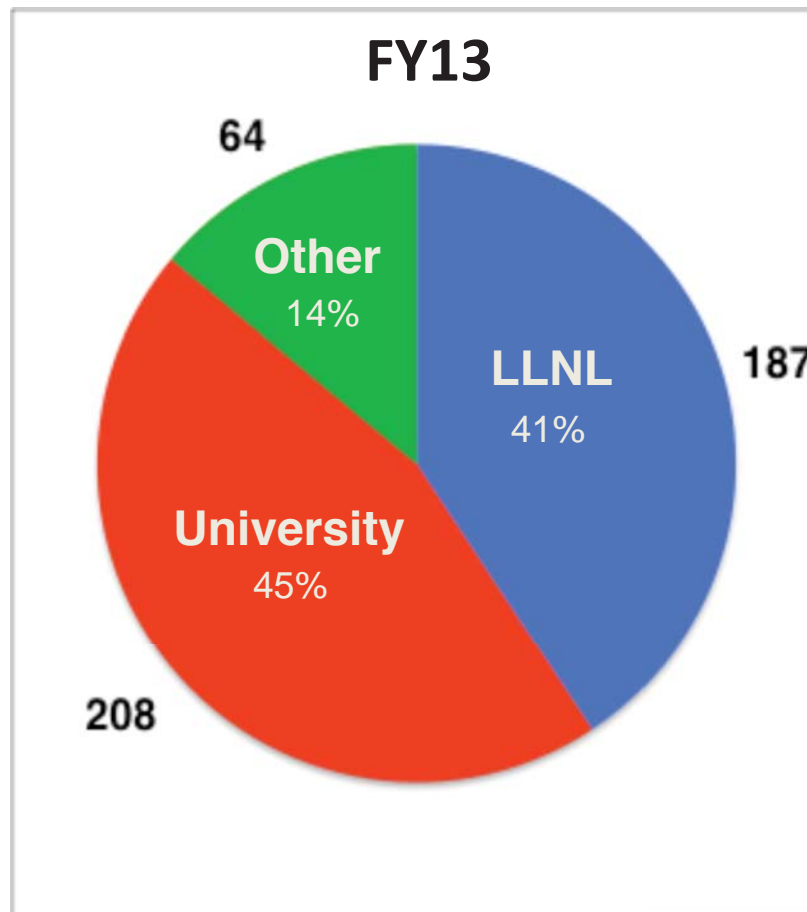
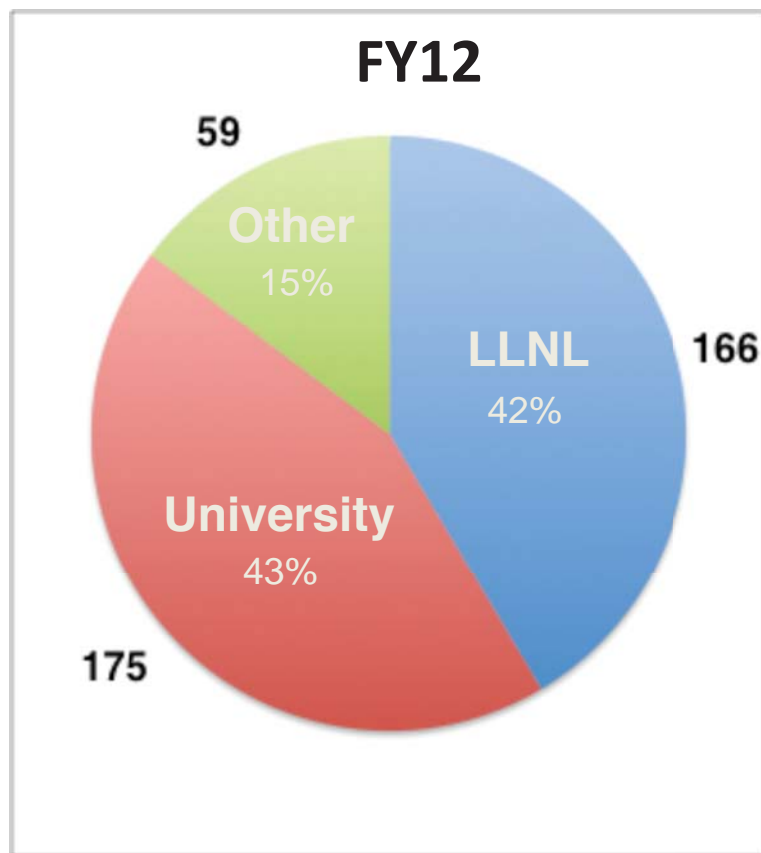
# Number of active JLF users continues to increase

By 2012 JLF had 400 users



# Number of active JLF users continues to increase

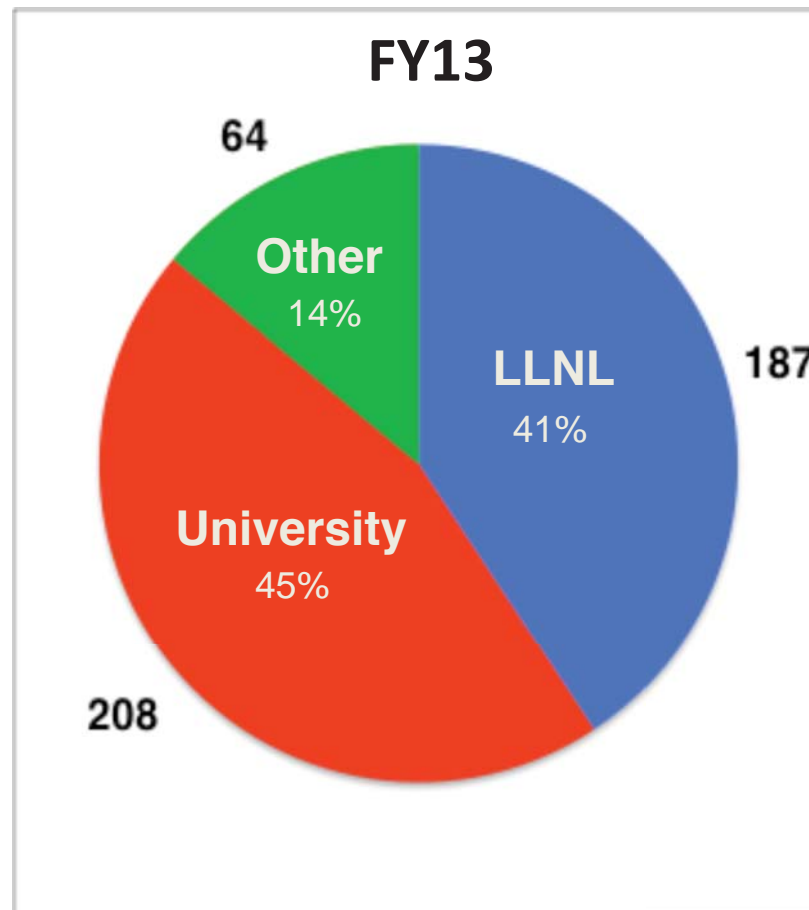
Now JLF has 459 users



# Number of student users also continues to increase

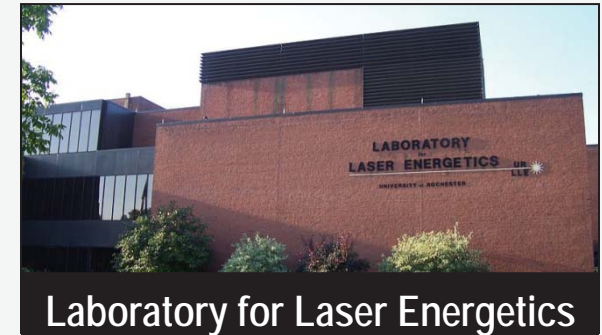
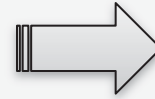
## Now JLF has 459 users

- FY12 (last UG meeting), **95** of 400 users were students
- Today the number is **117**
- 27 PhD's awarded since 2009 involving research at JLF
  - 11 became postdocs at LLNL
- 5 more finishing
  - 2 interviewing at LLNL
  - 1 offer at LLNL



# Jupiter is a development and proving ground for experiments and diagnostics that stage to larger facilities

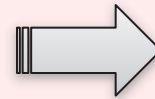
Chen (LLNL) – Positron Jets (Titan)  
Wark (Oxford) – Dynamic Deformation (Janus)  
Koenig (LULI) – WDM EOS (Titan)  
Multiple Users – Fast Ignition Studies, High-Pressure EOS,  
Thomson Scattering, X-ray Source Development,  
Detector Development



Chen (LLNL) – Pair Plasmas (Titan)  
Gregori (Oxford) – Collisionless Shocks (Titan)  
Falcone (UCB) – Thomson Scattering (Titan, Janus)  
Collins Group (LLNL) – Planetary Science, EOS (Janus)  
Lowry/Baker (LLNL) – Ultrafast Detectors (Callisto)  
NIF/NSTec/GA – X-ray Detector Qualification (COMET)



Hoarty (AWE) – High-Temperature  
Opacity/EOS (Titan)



# Jupiter has had 112 peer-reviewed publications since 2008; 24 in 2012



## ARTICLE

Received 10 Jul 2012 | Accepted 23 Oct 2012 | Published xx xxx 2012

DOI: 10.1038/ncomms2252

### Nanosecond white-light Laue diffraction measurements of dislocation microstructure in shock-compressed single-crystal copper

JOURNAL OF GEOPHYSICAL RESEARCH, VOL. 117, E09009, doi:10.1029/2012JE004082, 2012

### Shock vaporization of silica and the thermodynamics of planetary impact events

R. G. Kraus,<sup>1</sup> S. T. Stewart,<sup>1</sup> D. C. Swift,<sup>1</sup> C. A. Bolme,<sup>2</sup> R. F. Smith,<sup>2</sup> S. Hamel,<sup>2</sup> B. D. Hammel,<sup>2</sup> D. K. Spaulding,<sup>4</sup> D. G. Hicks,<sup>2</sup> J. H. Eggert,<sup>2</sup> and G. W. Collins<sup>2</sup>

Received 13 March 2012; revised 17 August 2012; accepted 18 August 2012; published 28 September 2012.

[1] The most energetic planetary collision/astation shock pressures that result in abundant melting and vaporization. Accurate predictions of the extent of melting and vaporization require knowledge of vast regions of the phase diagrams of the constituent materials. To reach the liquid-vapor phase boundary of silica, we conducted uniaxial shock-and-release experiments, where quartz was shocked to a state sufficient to initiate vaporization upon isentropic decompression (hundreds of GPa). The apparent temperature of the decompressing fluid was measured with a streaked optical pyrometer, and the bulk density was inferred by stagnation onto a standard window. To interpret the observed post-shock temperatures, we developed a model for the apparent temperature of a material isentropically decompressing through the liquid-vapor coexistence region. Using published thermodynamic data, we revised the liquid-vapor boundary for silica and calculated the entropy on the quartz Hugoniot. The silica post-shock temperature measurements, up to entropies beyond the critical point, are in excellent qualitative agreement with the predictions from the decompressing two-phase mixture model.

Shock-and-release experiments provide an accurate measurement of the temperature on the phase boundary for entropies below the critical point, with increasing uncertainties near and above the critical point entropy. Our new criteria for shock-induced vaporization of quartz are much lower than previous estimates, primarily because of the revised entropy on the Hugoniot. As the thermodynamics of other silicates are expected to be similar to quartz, vaporization is a significant process during high-velocity planetary collisions.

Keywords: Kraus, R. G., et al. (2012), Shock vaporization of silica and the thermodynamics of planetary impact events, *J. Geophys. Res.*, 117, E09009, doi:10.1029/2012JE004082.

1Institut für Kernphysik, Technische Universität Darmstadt, D-64289 Darmstadt, Germany

2Lawrence Livermore National Laboratory, Livermore, California 94550, USA

3Fachbereich Physik, Kaiserslautern, D-67661 Kaiserslautern, Germany

4Lawrence Livermore National Laboratory, Livermore, California 94550, USA

Correspondence to: R. G. Kraus, rkraus@livermore.gov

© 2012 American Institute of Physics

0002-6750/12/11709009-11\$12.00

This article is a U.S. Government work and, as such, is in the public domain in the United States of America.

© 2012 American Institute of Physics



### The principal shock

H. E. Lorenzana,<sup>2</sup> and J. H. Eggert,<sup>2</sup> *Lawrence Livermore National Laboratory, Livermore, California 94550, USA*

Received 10 July 2012; accepted 23 October 2012; published 15 October 2012

© 2012 American Institute of Physics

PRL 109, 145006 (2012) PHYSICAL REVIEW LETTERS week ending 5 OCTOBER 2012

### Dynamics of Relativistic Laser-Plasma Interaction on Solid Targets

Y. Ping,<sup>1</sup> A. J. Kemp,<sup>1</sup> L. Divol,<sup>1</sup> M. H. Key,<sup>1</sup> P. K. Patel,<sup>1</sup> K. U. Akli,<sup>1</sup> F. N. Beg,<sup>3</sup> S. Chawla,<sup>3</sup> C. D. Chen,<sup>1</sup> R. R. Freeman,<sup>4</sup> D. Hey,<sup>1</sup> D. P. Higginson,<sup>1</sup> L. C. Jarrott,<sup>1</sup> G. E. Kemp,<sup>4</sup> A. Link,<sup>4</sup> H. S. McLean,<sup>1</sup> H. Sawada,<sup>2</sup> R. B. Stephens,<sup>2</sup> D. Turnbull,<sup>5</sup> B. Wesleyover,<sup>2</sup> and S. C. Wilks<sup>1</sup>

<sup>1</sup>Lawrence Livermore National Laboratory, Livermore, California 94550, USA  
<sup>2</sup>General Atomics, San Diego, California 92186, USA  
<sup>3</sup>Department of Mechanical and Aerospace Engineering, University of California-San Diego, La Jolla, California 92093, USA  
<sup>4</sup>College of Mathematical and Physical Sciences, Ohio State University, Columbus, Ohio 43210, USA  
<sup>5</sup>Department of Mechanical and Aerospace Engineering, Princeton University, Princeton, New Jersey 08544, USA

(Received 6 May 2011; published 5 October 2012)

A novel time-resolved diagnostic is used to record the critical surface motion during picosecond-scale relativistic laser interaction with a solid target. Single-shot measurements of the specular light show a redshift decreasing with time during the interaction, corresponding to a slowing-down of the hole boring process into overense plasma. On-shot full characterization of the laser pulse enables simulation of the experiment without any free parameters. Two-dimensional particle-in-cell simulations yield redshifts that agree with the data, and support a simple explanation of the slowing-down of the critical surface based on momentum conservation between ions and reflected laser light.

DOI: 10.1103/PhysRevLett.109.145006 PACS numbers: 52.38-*t*, 52.70-*Ny*

PRL 108, 065701 (2012) PHYSICAL REVIEW LETTERS week ending 10 FEBRUARY 2012

### Evidence for a Phase Transition in Silicate Melt at Extreme Pressure and Temperature Conditions

D. K. Spaulding,<sup>1,2</sup> R. S. McWilliams,<sup>4</sup> R. Jeanloz,<sup>1</sup> J. H. Eggert,<sup>3</sup> P. M. Celliers,<sup>2</sup> D. G. Hicks,<sup>2</sup> G. W. Collins,<sup>2</sup> and R. F. Smith<sup>1</sup>

<sup>1</sup>Department of Earth and Planetary Science, University of California, Berkeley, California 94720-4767, USA  
<sup>2</sup>Department of Astronomy and Miller Institute for Basic Research in Science, University of California, Berkeley, California 94720-4767, USA  
<sup>3</sup>Shock Physics Group, Lawrence Livermore National Laboratory, Livermore, California 94550, USA  
<sup>4</sup>Geophysical Laboratory, Carnegie Institution of Washington, 3251 Branch Road Northwest, Washington, D. C. 20015, USA and Howard University, 2400 Sixth Street NW, Washington, D. C. 20059, USA

(Received 31 August 2011; published 8 February 2012)

Laser-driven shock compression experiments reveal the presence of a phase transition in MgSiO<sub>3</sub> over the pressure-temperature range 300–400 GPa and 10 000–16 000 K, with a positive Clapeyron slope and a volume change of ~6.3 (± 2.0) percent. The observations are most readily interpreted as an abrupt liquid-liquid transition in a silicate composition representative of terrestrial planetary mantles, implying potentially significant consequences for the thermal-chemical evolution of extraterrestrial planetary interiors. In addition, the present results extend the Hugoniot equation of state of MgSiO<sub>3</sub> single crystal and glass to 500 GPa.

DOI: 10.1103/PhysRevLett.108.065701 PACS numbers: 64.70.Ja, 62.50.-p, 64.30.Bk, 91.45.Bg

PHYSICAL REVIEW E 86, 065402(R) (2012)

### Laser light to fast electrons in cone-guided fast ignition

R. F. Smith,<sup>1</sup> M. Storm,<sup>1</sup> M. Fatenejad,<sup>2</sup> D. Lamb,<sup>2</sup> and R. R. Freeman<sup>1</sup>  
<sup>1</sup>State University, Columbus, Ohio 43210, USA  
<sup>2</sup>Astronomy & Astrophysics, University of Chicago, Chicago, Illinois 60637, USA

(Received 14 August 2012; published 28 December 2012)

We use to investigate the energy coupling efficiency of laser light to fast electrons in a plasma. We present experimental and simulation results demonstrating the efficiency of placing the cone in a surrounding high density plasma as well as the

### Phase Transformations and Metallization of Magnesium Oxide at High Pressure and Temperature

R. Stewart McWilliams,<sup>1,2,3</sup> Dylan K. Spaulding,<sup>1,3</sup> Jon H. Eggert,<sup>4</sup> Peter M. Celliers,<sup>4</sup> Damien G. Hicks,<sup>4</sup> Raymond F. Smith,<sup>4</sup> Gilbert W. Collins,<sup>4</sup> Raymond Jeanloz<sup>1,2,3</sup>

Magnesium oxide (MgO) is representative of the rocky materials comprising the mantles of terrestrial

PHYSICAL REVIEW B 86, 245204 (2012)

### Orientation and rate dependence in high strain-rate compression of single-crystal silicon

R. F. Smith,<sup>1</sup> R. W. Minich,<sup>1</sup> R. E. Rudd,<sup>1</sup> J. H. Eggert,<sup>1</sup> C. A. Bolme,<sup>2</sup> S. L. Bryggow,<sup>3</sup> A. M. Jones,<sup>4</sup> and G. W. Collins<sup>1</sup>

<sup>1</sup>Lawrence Livermore National Laboratory, P.O. Box 808, Livermore, California 94550, USA  
<sup>2</sup>Los Alamos National Laboratory, P.O. Box 1663, Los Alamos, New Mexico 87545, USA  
<sup>3</sup>CEA, DAM, DIF, F-91297 Arpajon, France

(Received 6 August 2012; published 17 December 2012)

High strain-rate ( $\dot{\epsilon} \sim 10^6 - 10^9 \text{ s}^{-1}$ ) compression of single crystal Si reveals strong orientation- and rate-dependent precursor stresses. At these high compression rates, the peak elastic stress,  $\sigma_{e,peak}$ , for Si [100], [110], and [111] exceeds twice the Hugoniot elastic limit. Near the loading surface, the rate at which Si evolves from uniaxial compression to a three-dimensional relaxed state is exponentially dependent on  $\sigma_{e,peak}$  and independent of initial crystal orientation. At later times, the high elastic wave speed results in a temporal decoupling of the elastic precursor from the main inelastic wave. A rapid high- $\dot{\epsilon}$  increase in the measured elastic stress at the onset of inelastic deformation is consistent with a transition from dislocation flow mediated by thermal activation to a phonon drag regime.

DOI: 10.1103/PhysRevB.86.245204 PACS number(s): 61.72.Ff, 62.20.F-, 62.20.D-

PRL 108, 115004 (2012) PHYSICAL REVIEW LETTERS week ending 16 MARCH 2012

### Hot Electron Temperature and Coupling Efficiency Scaling with Prepulse for Cone-Guided Fast Ignition

T. Ma,<sup>1,2</sup> H. Sawada,<sup>2</sup> P. K. Patel,<sup>1</sup> C. D. Chen,<sup>1</sup> L. Divol,<sup>1</sup> D. P. Higginson,<sup>1,2</sup> A. J. Kemp,<sup>1</sup> M. H. Key,<sup>1</sup> D. J. Larson,<sup>1</sup> S. Le Pape,<sup>1</sup> A. Link,<sup>1,2</sup> A. G. MacPhee,<sup>1</sup> R. S. McLean,<sup>1</sup> Y. Ping,<sup>1</sup> R. B. Stephens,<sup>2</sup> S. C. Wilks,<sup>1</sup> and P. N. Beg<sup>3</sup>

<sup>1</sup>Lawrence Livermore National Laboratory, Livermore, California 94550, USA  
<sup>2</sup>University of California-San Diego, La Jolla, California 92093, USA  
<sup>3</sup>The Ohio State University, Columbus, Ohio 43210, USA  
<sup>4</sup>General Atomics, San Diego, California 92186, USA

(Received 3 December 2011; published 16 March 2012)

The effect of increasing prepulse energy levels on the energy spectrum and coupling into forward-going electrons is evaluated in a cone-guided fast-ignition relevant geometry using cone-wire targets irradiated with a high intensity ( $10^{20} \text{ W/cm}^2$ ) laser pulse. Hot electron temperature and flux are inferred from  $K\alpha$  images and yields using hybrid particle-in-cell simulations. A two-temperature distribution of hot electrons was required to fit the full profile, with the ratio of energy in a higher energy (MeV) component increasing with a larger prepulse. As prepulse energies were increased from 8 mJ to 1 J, overall coupling from laser to all hot electrons entering the wire was found to fall from 8.4% to 2.5% while coupling into only the 1–3 MeV electrons dropped from 0.57% to 0.03%.

DOI: 10.1103/PhysRevLett.108.115004 PACS numbers: 52.50.Jz, 52.38.Kd, 52.38.Mf, 52.70.La

and fusion burn-history measurements with  $\sim \text{ps}$  resolution. © 2012 American Institute of Physics. [http://dx.doi.org/10.1063/1.4729677]

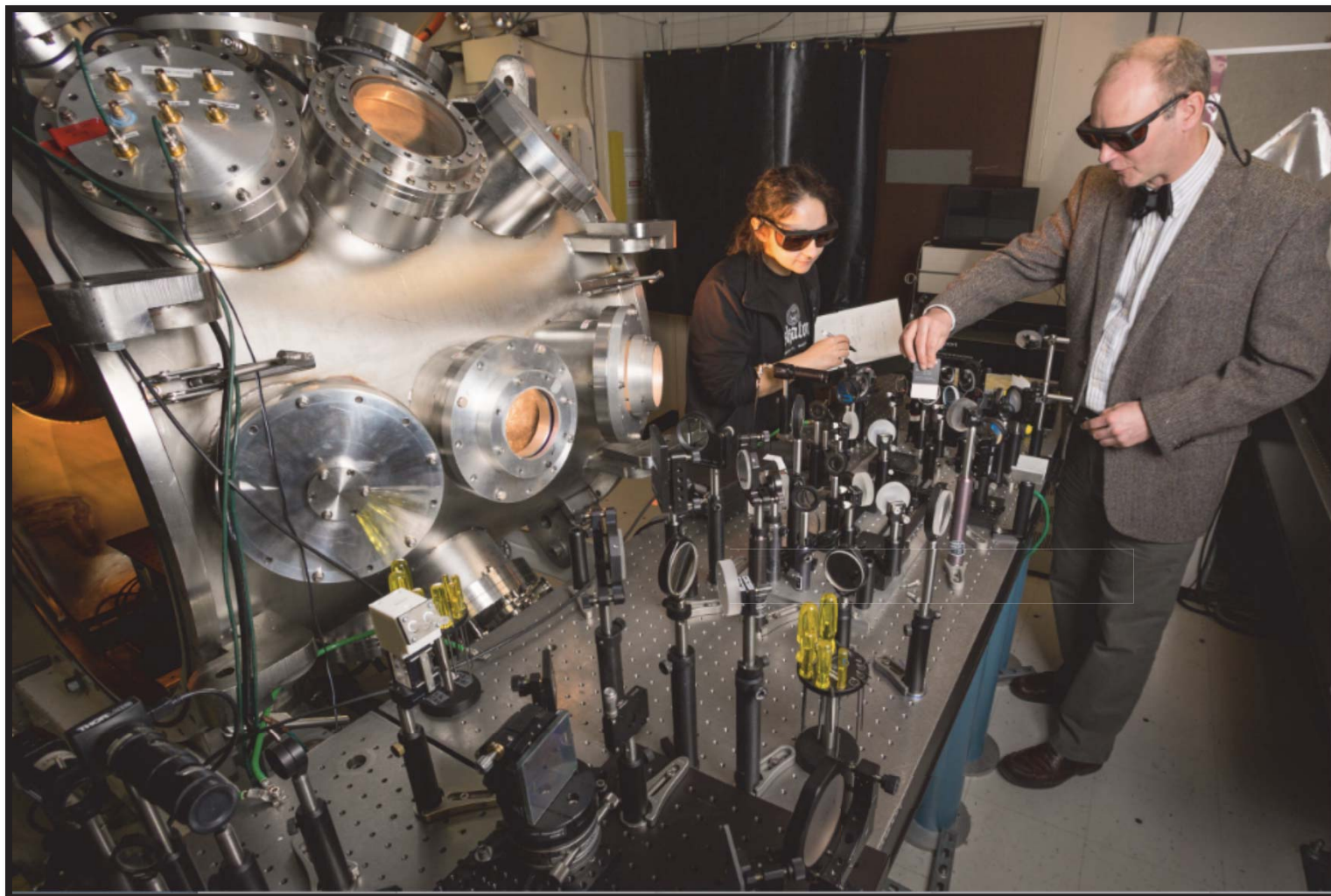
### An apparatus for the characterization of deuterium with inelastic neutron scattering

P. Davis,<sup>1</sup> T. Döppner,<sup>2</sup> S. H. Glenzer,<sup>3</sup> and J. H. Eggert<sup>4</sup>

<sup>1</sup>University of California Berkeley, Berkeley, CA 94720, USA  
<sup>2</sup>Lawrence Livermore National Laboratory, P.O. Box 808, Livermore, CA 94551, USA  
<sup>3</sup>Lawrence Livermore National Laboratory, P.O. Box 808, Livermore, CA 94551, USA  
<sup>4</sup>Lawrence Livermore National Laboratory, P.O. Box 808, Livermore, CA 94551, USA



# Recent highlights from Jupiter/Janus



# Recent highlights from Jupiter/Janus



# New results affecting planetary structure

JOURNAL OF GEOPHYSICAL RESEARCH, VOL. 117, E09009, doi:10.1029/2012JE004082, 2012

## Shock vaporization of silica and the thermodynamics of planetary impact events

R. G. Kraus,<sup>1</sup> S. T. Stewart,<sup>1</sup> D. C. Swift,<sup>2</sup> C. A. Bolme,<sup>3</sup> R. F. Smith,<sup>2</sup> S. Hamel,<sup>2</sup> B. D. Hammel,<sup>2</sup> D. K. Spaulding,<sup>4</sup> D. G. Hicks,<sup>2</sup> J. H. Eggert,<sup>2</sup> and G. W. Collins<sup>2</sup>

Received 15 March 2012; revised 17 August 2012; accepted 18 August 2012; published 28 September 2012.

[1] The most energetic planetary collisions attain shock pressures that result in abundant melting and vaporization. Accurate predictions of the extent of melting and vaporization require knowledge of vast regions of the phase diagrams of the constituent materials. To reach the liquid-vapor phase boundary of silica, we conducted uniaxial shock-and-release experiments, where quartz was shocked to a state sufficient to initiate vaporization upon isentropic decompression (hundreds of GPa). The apparent temperature of the decompressing fluid was measured with a streaked optical pyrometer, and the bulk density was inferred by stagnation onto a standard window. To interpret the observed post-shock temperatures, we developed a model for the apparent temperature of a material isentropically decompressing through the liquid-vapor coexistence region. Using published thermodynamic data, we revised the liquid-vapor boundary for silica and calculated the entropy on the quartz Hugoniot. The silica post-shock temperature measurements, up to entropies beyond the critical point, are in excellent qualitative agreement with the predictions from the decompressing two-phase mixture model. Shock-and-release experiments provide an accurate measurement of the temperature on the phase boundary for entropies below the critical point, with increasing uncertainties near and above the critical point entropy. Our new criteria for shock-induced vaporization of quartz are much lower than previous estimates, primarily because of the revised entropy on the Hugoniot. As the thermodynamics of other silicates are expected to be similar to quartz, vaporization is a significant process during high-velocity planetary collisions.

**Citation:** Kraus, R. G., et al. (2012), Shock vaporization of silica and the thermodynamics of planetary impact events, *J. Geophys. Res.*, 117, E09009, doi:10.1029/2012JE004082.

### 1. Introduction

[2] During the end stage of planet formation, the nebular gas disperses and mutual encounter velocities increase via gravitational stirring from the largest bodies. *N*-body simulations of this stage find typical collision velocities between protoplanets of one to a few times the two-body escape velocity [Agnor et al., 1999]. The kinetic energy of an impact is partially transferred to internal energy in the colliding bodies via passage of a strong shock wave. At the expected impact velocities of ~10 to a few tens of km s<sup>-1</sup> onto the growing planets, the internal energy increase is

sufficient to melt and vaporize a large fraction of the colliding bodies. However, the predicted degree of melting and vaporization for a specific impact scenario has great uncertainty that primarily arises from poorly-constrained equations of state (EOS).

[3] Accurate equations of state over a tremendous region of phase space are required to make predictions about the impact processes so prevalent during the formation of the solar system and its subsequent evolution. The last giant impact is invoked to explain the diverse characteristics of rocky and icy planets in the Solar System [e.g., Stewart and Leinhardt, 2012], including the large core of Mercury [Benz et al., 1988, 2007], formation of Earth's moon [Canup and Asphaug, 2001], Pluto's moons [Canup, 2005], and Haumea's moons and family members [Leinhardt et al., 2010]. In each case, the argument for a giant impact relies upon the details of the equations of state.

[4] Although equation of state theory is advancing rapidly, the generation of accurate and complete equations of state from first principles is still not feasible for most geologic materials. Planetary collisions are particularly challenging because of the need to understand both the extreme temperatures and high compression ratios achieved in the

<sup>1</sup>Department of Earth and Planetary Sciences, Harvard University, Cambridge, Massachusetts, USA.

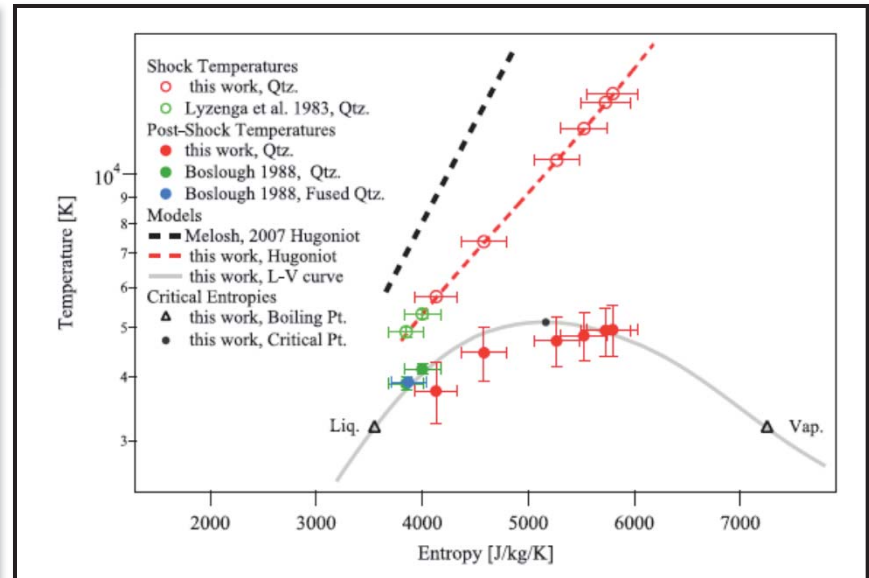
<sup>2</sup>Lawrence Livermore National Laboratory, Livermore, California, USA.

<sup>3</sup>Los Alamos National Laboratory, Los Alamos, New Mexico, USA.

<sup>4</sup>Department of Earth and Planetary Sciences, University of California, Berkeley, California, USA.

Corresponding author: R. G. Kraus, Department of Earth and Planetary Sciences, Harvard University, 20 Oxford St., Cambridge, MA 02138, USA. (rkraus@fas.harvard.edu)

©2012. American Geophysical Union. All Rights Reserved. 0148-0227/12/2012JE004082



- New liquid-vapor phase boundary
- New shock vaporization criteria
- Previous studies underestimated amount of vapor produced in planetary impacts

# New results affecting planetary structure

## REPORTS

(Fig. 3A). Pt deposition resulted in three distinct levels of contrast that reflect the surface height, with the lowest level being the original Au terraces (Fig. 3B). The same three-level structure was observed independently of deposition time up to 500 s (Fig. 3C). The middle contrast level corresponds to a high density of Pt islands that covered ~85% of the Au surface, with a step height of ~0.24 nm, consistent with XPS results. Inspection with a higher rendering contrast revealed a ~10% coverage of a second layer of small Pt islands with a step height ranging between 0.23 and 0.26 nm (Fig. 3D). Step positions associated with the flame-annealed substrate were preserved, with negligible expansion or overgrowth of the 2D Pt islands occurring beyond the original step edge. The lateral span of the Pt islands was  $2.02 \pm 0.38$  nm, corresponding to an area of  $4.23 \pm 1.97$  nm<sup>2</sup>. Incipient coalescence of the islands was constrained by surrounding (dark) narrow channels,  $2.1 \pm 0.25$  nm wide, that account for the remaining Pt-free portion of the first layer. The reentrant channels correspond to open Au terrace sites that were surrounded by adjacent Pt islands in what amounted to a huge increase in step density relative to the original substrate, the net geometric or electronic effect of which was to block further Pt deposition. The chemical nature of the inter-island region was assayed by exploiting the distinctive voltammetry of Pt and Au with respect to  $H_{\text{upd}}$  and oxide formation and reduction (fig. S2 and supplementary text).

Similar three-level Pt overlayers have been observed for monolayer films produced by molecular beam epitaxy (MBE) deposition at 0.05 monolayers/min (20). Pt-Au intermixing driven by the decrease in surface energy that accompanies Au surface segregation was evident. In the present work, Pt monolayer formation was effectively complete within 1 s, giving a growth rate three orders of magnitude greater than in the MBE-STM study. Exchange of the deposited Pt with the underlying Au substrate was expected to be less developed. However, intermixing and possible chemical contrast (i.e. the ligand effect) were evident on limited sections of the surface that were correlated with the original faulted geometry of the partially reconstructed Au surface. Upon lifting of the reconstruction, the excess Au atoms expelled mark the original fault location as linear 1D surface defects in the Pt overlayer (Fig. 3E). A simplified schematic of the self-terminating Pt deposition process in Fig. 3F describes how the  $H_{\text{upd}}$  accompanying incremental expansion of the 2D Pt islands can hinder the development of a second Pt layer, presumably by perturbation of the overlying water structure (17). This rapid process resulted in a much higher Pt island coverage than has been obtained by other methods, such as galvanic exchange reactions.

Because the saturated  $H_{\text{upd}}$  coverage is the agent of termination, reactivation for further Pt deposition was possible by removing the upd layer by sweeping or stepping the potential to positive values, e.g.,  $>+0.2 V_{\text{SCE}}$ , where negligible Pt dep-

osition occurs. Sequential pulsing between  $+0.4 V_{\text{SCE}}$  and  $-0.8 V_{\text{SCE}}$  enabled Pt monolayer deposition to be controlled in a digital manner. EQCM was used to track the mass gain, showing two net increments per cycle (Fig. 4A). We attributed the mass gain to a combination of Pt deposition [ $48 \text{ ng/cm}^2$  for a monolayer of Pt(111)], anion adsorption and desorption ( $41 \text{ ng/cm}^2$  for  $7 \times 10^{14} \text{ Cl}^-$  ion/cm<sup>2</sup>),  $117 \text{ ng/cm}^2$  for a 0.14 fractional coverage of  $\text{PtCl}_2^{2-}$  (7, 21), and coupling to other double-layer components such as water. The anionic mass increments were expected to be asymmetric for the first cycle on the Au surface, but once it was covered, subsequent cycles only involved Pt surface chemistry. After correcting for the electroactive surface area of the Au electrode ( $A_{\text{real}}/A_{\text{geometric}} = 1.2$ , derived from reductive desorption of Au oxide in perchloric acid), the net mass gain for each cycle indicates that a near-pseudomorphic layer of Pt was deposited. XPS analysis of Pt films grown in various deposition cycles gave remarkably good agreement with EQCM data (Fig. 4B). The ability to rapidly manipulate potential and double-layer structure, as opposed to the exchange of reactants, offers simplicity, substantially improved process efficiency, and far greater process speed than other surface-limited deposition methods.

### References and Notes

1. F. T. Wagner, R. Lakshmanan, M. F. Mathias, *J. Phys. Chem. Lett.* **1**, 2204 (2010).
2. M. K. Dole, *Nature* **486**, 43 (2012).
3. M. T. M. Koper, Ed., *Fuel Cell Catalysis: A Surface Science Approach* (Wiley, Hoboken, NJ, 2009).
4. V. R. Stamenkovic et al., *Nat. Mater.* **6**, 241 (2007).
5. R. R. Adzic et al., *Top. Catal.* **46**, 249 (2007).
6. T. Nishiyuki, J. Knig, *Islands, Mounds and Atoms: Patterns and Processes in Crystal Growth Far from Equilibrium* (Springer Series in Surface Science, V42, Springer, New York, 2003).

## Phase Transformations and Metallization of Magnesium Oxide at High Pressure and Temperature

R. Stewart McWilliams,<sup>1,2,†</sup> Dylan K. Spaulding,<sup>3,†</sup> Jon H. Eggert,<sup>4</sup> Peter M. Celliers,<sup>4</sup> Damien G. Hicks,<sup>4</sup> Raymond F. Smith,<sup>4</sup> Gilbert W. Collins,<sup>4</sup> Raymond Jeanloz<sup>1,5</sup>

Magnesium oxide (MgO) is representative of the rocky materials comprising the mantles of terrestrial planets, such that its properties at high temperatures and pressures reflect the nature of planetary interiors. Shock-compression experiments on MgO to pressures of 1.4 terapascals (TPa) reveal a sequence of two phase transformations: from B1 (sodium chloride) to B2 (cesium chloride) crystal structures above 0.36 TPa, and from electrically insulating solid to metallic liquid above 0.60 TPa. The transitions exhibit large latent heats that are likely to affect the structure and evolution of super-Earths. Together with data on other oxide liquids, we conclude that magmas deep inside terrestrial planets can be electrically conductive, enabling magnetic field-producing dynamo action within oxide-rich regions and blurring the distinction between planetary mantles and cores.

Magnesium oxide (MgO) is among the simplest oxides constituting the rocky mantles of terrestrial planets such as

Earth and the cores of Jupiter and other giant planets. Present in Earth's mantle as an end-member component of the mineral (Mg,Fe)O magnesio-wüstite,

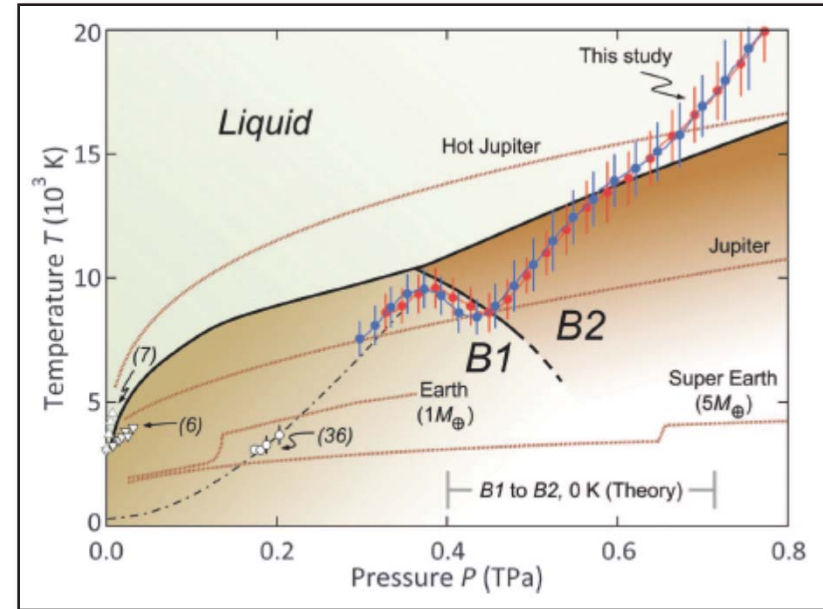
7. H. F. Walbel, M. Kleinert, L. A. Kibler, D. M. Kolb, *Electrochim. Acta* **47**, 1461 (2002).
8. T. Kondo et al., *Electrochim. Acta* **55**, 8302 (2010).
9. I. Bakos, S. Saabo, T. Pajkossy, *J. Solid State Electrochem.* **15**, 2453 (2011).
10. S. R. Brankovic, J. X. Wang, R. R. Adzic, *Surf. Sci.* **474**, 1173 (2001).
11. D. Gokcen, S.-E. Bae, S. R. Brankovic, *Electrochim. Acta* **56**, 5545 (2011).
12. B. W. Gregory, J. L. Stickney, *J. Electroanal. Chem.* **300**, 543 (1991).
13. A. J. Gregory, W. Lewason, R. E. Nettle, R. Le Penven, D. Pletcher, *J. Electroanal. Chem.* **399**, 105 (1995).
14. See supplementary materials on Science Online.
15. N. Garcia-Araza, V. Climent, E. Herrero, J. Felix, J. Lipkowski, *J. Electroanal. Chem.* **582**, 76 (2005).
16. D. Stamenik, D. Viplak, D. van der Vliet, V. Stamenkovic, N. M. Markovic, *Electrochim. Commun.* **10**, 1602 (2008).
17. T. Roman, A. Groß, Structure of water layers on hydrogen-covered Pt electrodes. *Catal. Today*; <http://dx.doi.org/10.1016/j.cattod.2012.06.001> (2012).
18. G. Jerkiewicz, G. Vatankhah, S. Tanaka, J. Lesard, *Langmuir* **27**, 4220 (2011).
19. P. J. Cumpson, M. P. Seah, *Surf. Interface Anal.* **25**, 430 (1997).
20. M. O. Pedersen et al., *Surf. Sci.* **426**, 395 (1999).
21. Y. Nagahara et al., *J. Phys. Chem. B* **308**, 3224 (2004).

**Acknowledgments:** We thank J. J. Mallet for his early observations on the difficulty of electrodepositing Pt films at negative potentials. This work was supported by NIST-Material Measurement Laboratory programs. The x-ray photoelectron spectrometer was provided by NIST-American Recovery and Reinvestment Act funds. Y.L. thanks the NIST-National Research Council Postdoctoral Fellowship Program for support. NIST has filed a provisional patent application (Atomic Layer Deposition of Pt from Aqueous Solutions) based on this work.

### Supplementary Materials

[www.sciencemag.org/quickcontent/full/338/6112/1327/DC1](http://www.sciencemag.org/quickcontent/full/338/6112/1327/DC1)  
Materials and Methods  
Supplementary Text  
Figs. S1 and S2  
References (22–26)

16 August 2012; accepted 17 October 2012  
10.1126/science.1228925



- Established solid-solid phase transition for the first time
- Metallization above 6 Mbar – dynamo effect possible in deep mantles
- Unexpectedly large latent heats

Expts at JLF and Omega

# New results affecting planetary structure

PRL 108, 065701 (2012)

PHYSICAL REVIEW LETTERS

week ending  
10 FEBRUARY 2012

## Evidence for a Phase Transition in Silicate Melt at Extreme Pressure and Temperature Conditions

D. K. Spaulding,<sup>1,\*</sup> R. S. McWilliams,<sup>4</sup> R. Jeanloz,<sup>1,2</sup> J. H. Eggert,<sup>3</sup>  
P. M. Celliers,<sup>3</sup> D. G. Hicks,<sup>3</sup> G. W. Collins,<sup>3</sup> and R. F. Smith<sup>3</sup>

<sup>1</sup>Department of Earth and Planetary Science, University of California, Berkeley, California 94720-4767, USA

<sup>2</sup>Department of Astronomy and Miller Institute for Basic Research in Science,  
University of California, Berkeley, California 94720-4767, USA

<sup>3</sup>Shock Physics Group, Lawrence Livermore National Laboratory, Livermore, California 94550, USA

<sup>4</sup>Geophysical Laboratory, Carnegie Institution of Washington, 5251 Broad Branch Road Northwest, Washington, D.C. 20015, USA  
and Howard University, 2400 Sixth Street NW, Washington, D.C. 20059, USA.

(Received 31 August 2011; published 8 February 2012)

Laser-driven shock compression experiments reveal the presence of a phase transition in  $\text{MgSiO}_3$  over the pressure-temperature range 300–400 GPa and 10 000–16 000 K, with a positive Clapeyron slope and a volume change of  $\sim 6.3 (\pm 2.0)$  percent. The observations are most readily interpreted as an abrupt liquid-liquid transition in a silicate composition representative of terrestrial planetary mantles, implying potentially significant consequences for the thermal-chemical evolution of extrasolar planetary interiors. In addition, the present results extend the Hugoniot equation of state of  $\text{MgSiO}_3$  single crystal and glass to 950 GPa.

DOI: 10.1103/PhysRevLett.108.065701

PACS numbers: 64.70.Ja, 62.50.-p, 64.30.Jk, 91.45.Bg

Crystallographic phase transformations in the mineral phases constituting the terrestrial mantle have long been recognized for their role in governing the structure and geodynamic evolution of the Earth's interior [1–4]. Here, we present direct experimental evidence that similar, pressure-induced phase changes can occur in silicate liquids (magmas) at the extreme conditions characteristic of the interiors of several Earth-mass extrasolar planets (super-Earths) and the type of giant impact events inherent to planetary formation (pressures of many hundred GPa and temperatures exceeding  $1 \text{ eV} \approx 11\,000 \text{ K}$ ). Experimental observations of such “first-order” liquid-liquid transitions are so far limited to a few cases, notably that of phosphorous [5–7]. Because of the key role that melts play in planetary evolution, pressure-induced liquid-liquid phase separation in silicate magmas may represent a previously unrecognized but important mechanism for global-scale chemical differentiation and may also influence the thermal transport and convective processes that govern the formation of a mantle and core early in planetary history.

Experiments were carried out at the Janus and OMEGA laser facilities (Lawrence Livermore National Lab and University of Rochester Laboratory for Laser Energetics). A 1–2 ns laser pulse of intensity  $\sim 10^{13} \text{ W/cm}^2$  was used to generate optically reflecting, decaying shock waves in  $\text{MgSiO}_3$  glass and crystalline (enstatite) samples. As the wave decays in time, a continuum of pressure-temperature shock states can be documented in a single experiment. Spatially and temporally resolved ( $\sim 10 \mu\text{m}/\text{pixel}$  and 100 ps, respectively) velocity interferometry [8,9] and optical pyrometry [10,11] were used to characterize the evolution of shock velocity ( $U_s$ ) and temperature ( $T$ ) (Fig. 1).

Similarly, the optical reflectivity at 532 nm ( $R$ ) was obtained from the interferometry data by comparison with an unshocked Al reference. Because conservation of mass, momentum, and energy are obeyed at the shock front, pressure ( $P$ ) and specific volume ( $V$ ) can be determined from the shock velocity using the Rankine-Hugoniot equations [12]. We thus derive the pressure-density equation of state (EOS) and corresponding temperature and specific

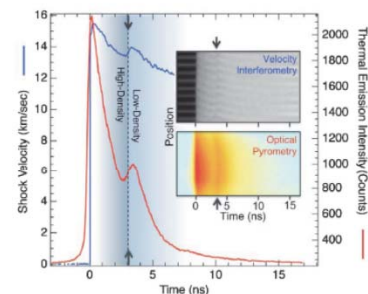
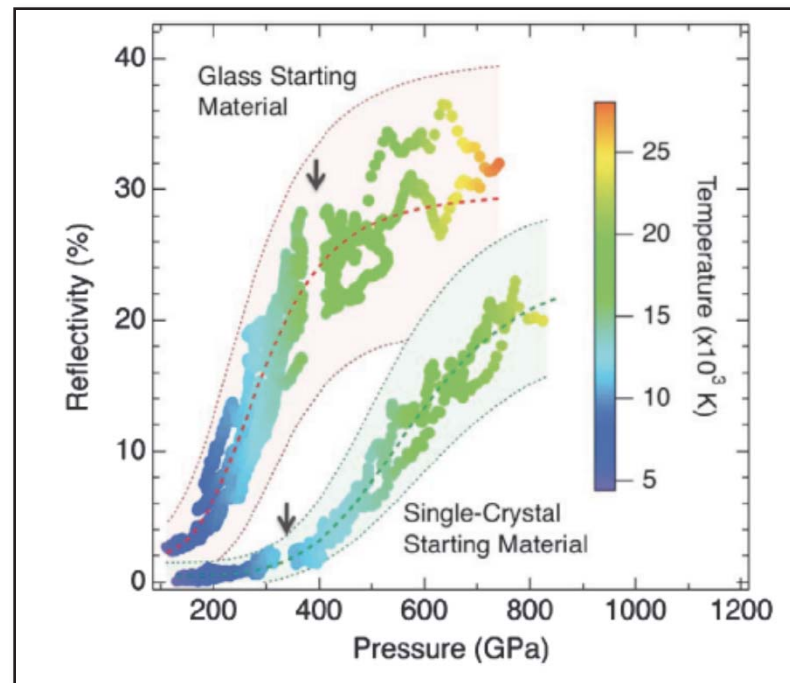


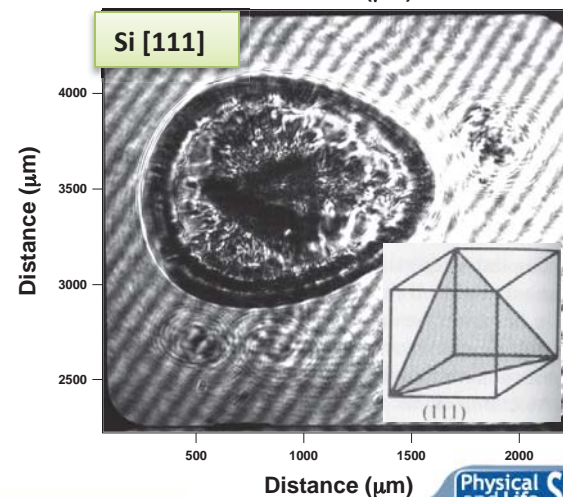
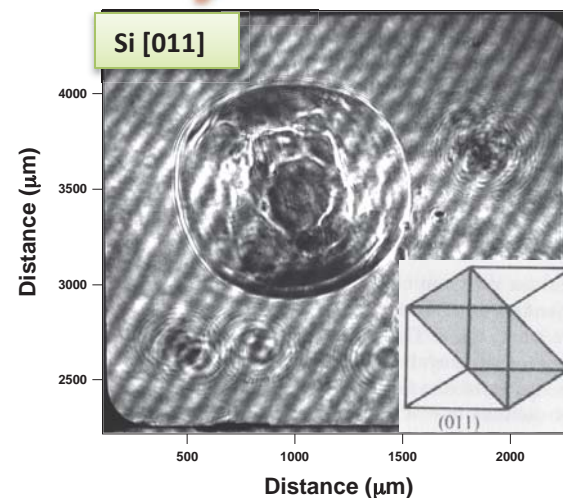
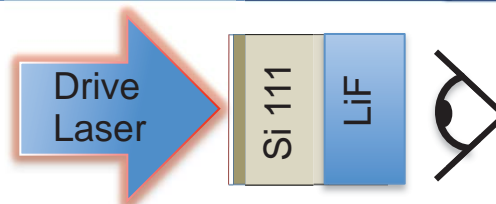
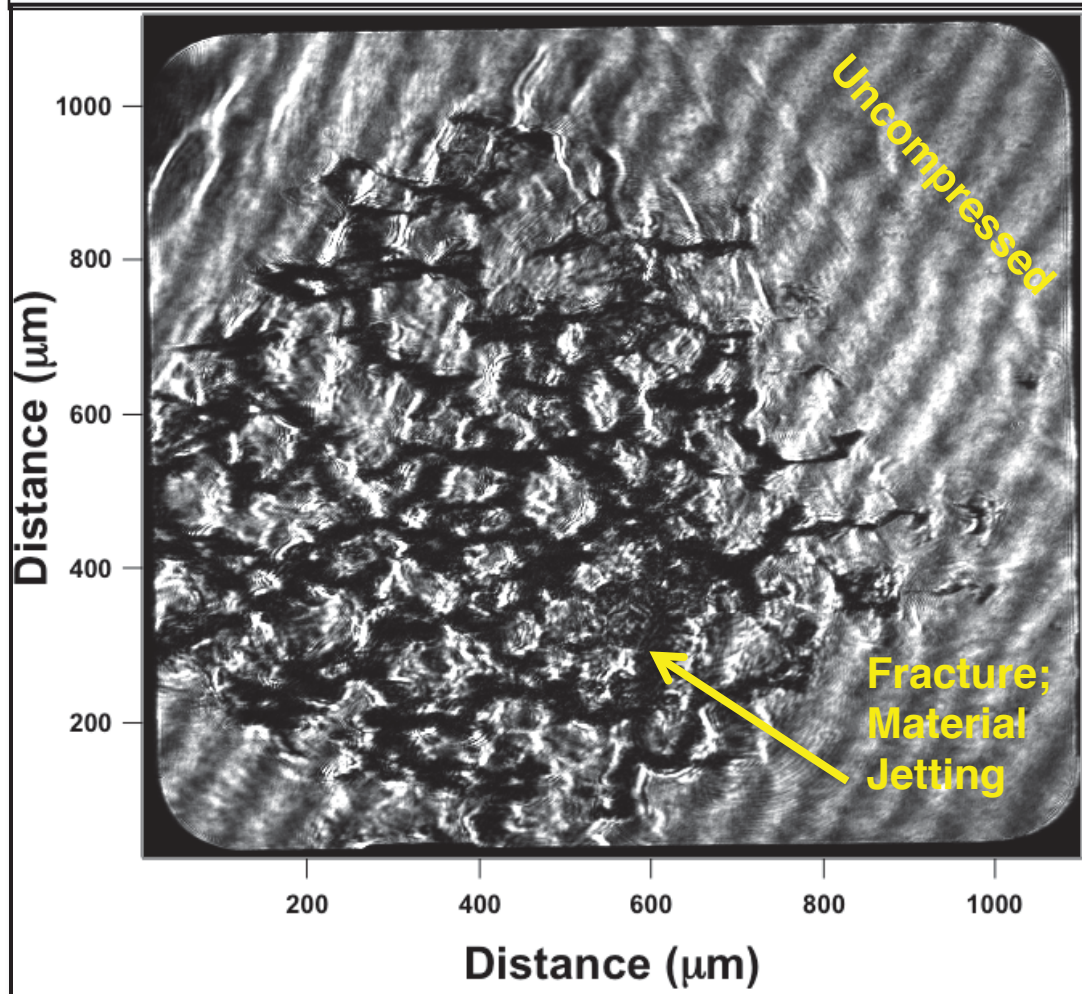
FIG. 1 (color). An example of data from a single experiment performed with crystalline starting material shows simultaneous reversals in shock velocity and temperature as a function of time as the Hugoniot crosses the phase transition (visible between 2 and 4 ns, as indicated by arrows and the dashed line). Inset: arrows indicate the transition in the raw data images, from which the profiles in the main figure are extracted.



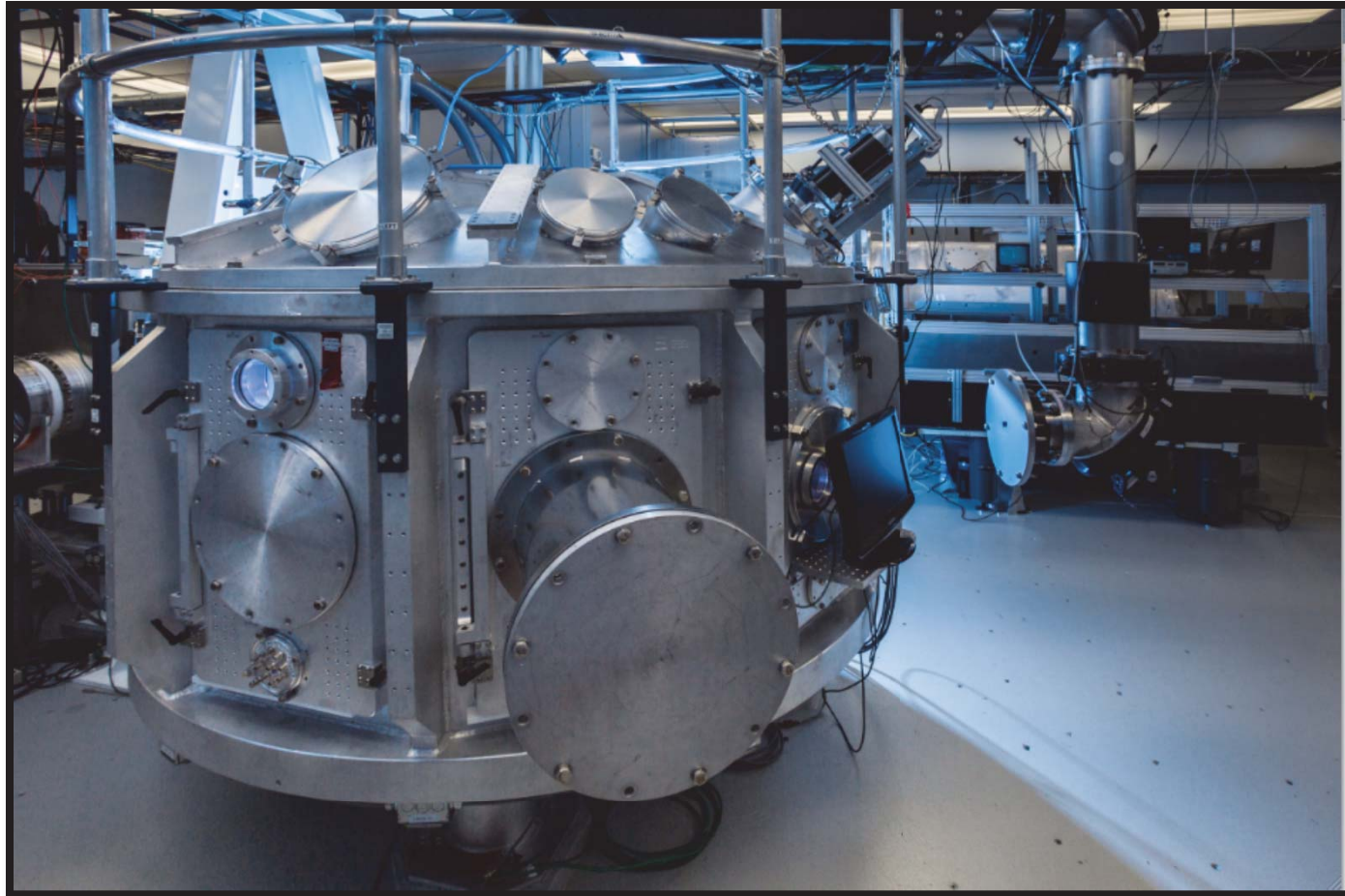
- Liquid-liquid phase transition discovered above 3 Mbar
- Distinguishes glass and single-crystal
- Extends  $\text{MgSiO}_3$  EOS to 9.5 Mbar

# New results utilizing JAVELIN

## 2D VISAR Image



# Recent highlights from Jupiter/Titan



# New results on fast ignition

PRL 108, 115004 (2012)

PHYSICAL REVIEW LETTERS

week ending  
16 MARCH 2012

## Hot Electron Temperature and Coupling Efficiency Scaling with Prepulse for Cone-Guided Fast Ignition

T. Ma,<sup>1,2</sup> H. Sawada,<sup>2</sup> P.K. Patel,<sup>1</sup> C. D. Chen,<sup>1</sup> L. Divol,<sup>1</sup> D. P. Higginson,<sup>1,2</sup> A. J. Kemp,<sup>1</sup> M. H. Key,<sup>1</sup> D. J. Larson,<sup>1</sup> S. Le Pape,<sup>1</sup> A. Link,<sup>1,3</sup> A. G. MacPhee,<sup>1</sup> H. S. McLean,<sup>1</sup> Y. Ping,<sup>1</sup> R. B. Stephens,<sup>4</sup> S. C. Wilks,<sup>1</sup> and F. N. Beg<sup>2</sup>

<sup>1</sup>Lawrence Livermore National Laboratory, Livermore, California 94550, USA

<sup>2</sup>University of California-San Diego, La Jolla, California 92093, USA

<sup>3</sup>The Ohio State University, Columbus, Ohio 43210, USA

<sup>4</sup>General Atomics, San Diego, California 92186, USA

(Received 3 December 2011; published 16 March 2012)

The effect of increasing prepulse energy levels on the energy spectrum and coupling into forward-going electrons is evaluated in a cone-guided fast-ignition relevant geometry using cone-wire targets irradiated with a high intensity ( $10^{20}$  W/cm<sup>2</sup>) laser pulse. Hot electron temperature and flux are inferred from  $K\alpha$  images and yields using hybrid particle-in-cell simulations. A two-temperature distribution of hot electrons was required to fit the full profile, with the ratio of energy in a higher energy (MeV) component increasing with a larger prepulse. As prepulse energies were increased from 8 mJ to 1 J, overall coupling from laser to all hot electrons entering the wire was found to fall from 8.4% to 2.5% while coupling into only the 1–3 MeV electrons dropped from 0.57% to 0.03%.

DOI: 10.1103/PhysRevLett.108.115004

PACS numbers: 52.50.Jm, 52.38.Kd, 52.38.Mr, 52.70.La

Fast Ignition (FI) [1,2] is an approach to inertial confinement fusion (ICF), in which a precompressed deuterium-tritium fuel is rapidly driven to ignition by an external heat source. This scheme can ignite lower density fuel leading, in principle, to higher gains than possible with conventional ignition. In the reentrant cone approach to FI, a hollow cone is embedded in the fuel capsule to provide an open evacuated path free of coronal plasma for an intense laser beam to generate a flux of energetic electrons at the tip of the cone which can then propagate to the compressed fuel core. However, the presence of preformed plasma in the cone, arising from the inherent laser prepulse which ablates the inner cone wall, can strongly affect the spatial, energy-spectral, and angular characteristics of these laser-generated hot electrons and thus the efficiency with which their energy can be coupled to the core.

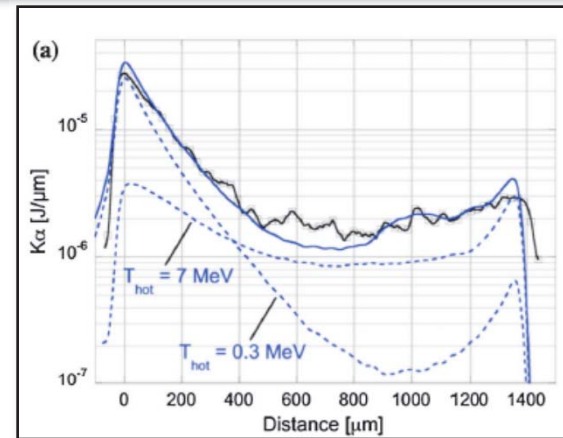
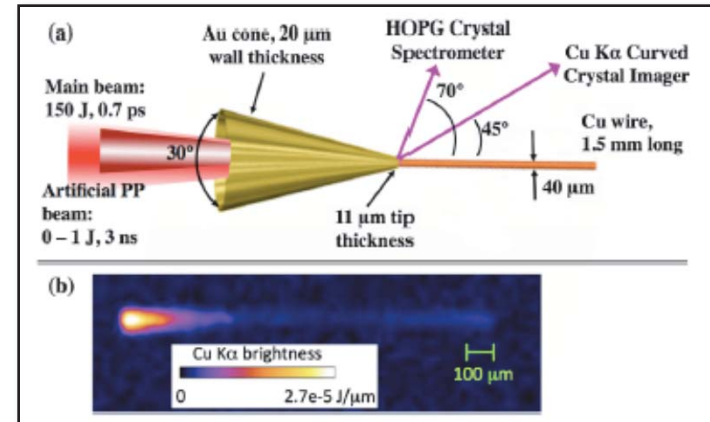
Previous works by Baton *et al.* [3] and Van Woerkom *et al.* [4] showed that significant prepulse could have a detrimental effect on coupling beyond the cone tip. MacPhee *et al.* [5] demonstrated that even a small prepulse could result in significant filamentation of the laser beam in the preplasma, limiting the penetration of the laser, and accelerating energetic electrons transversely. These results were achieved using either imaging of  $K\alpha$  x-ray emission from the cone target itself or measuring the intensity of the  $K\alpha$  spot in a region beyond the cone tip. However, while these techniques provided a spatial distribution of  $K\alpha$  in various areas of the interaction, no spectral information regarding the electron flux could be inferred. Comparisons of preplasma versus no preplasma conditions by Baton *et al.* were achieved by doubling the fundamental laser frequency to create a high contrast. This provided a clean interaction surface for the main laser, but complicated the

comparison, as the absorption mechanisms would be different for the very different  $\lambda^2$ . In the MacPhee *et al.* study, electrons were electrostatically confined within the isolated cone target. The significant amount of recirculation of the hot electrons within the cone walls and plasma allows only limited conclusion of the electron source at the cone tip in either the experiment or simulations.

In this Letter, we present the first quantitative scaling of coupling as a function of prepulse in an intense laser-cone interaction. Through the use of cone-wire targets [6], we demonstrate the existence of a two-temperature hot electron distribution within the target and characterize its flux and energy spectrum entering a 40  $\mu\text{m}$  diameter wire at the cone tip, and correlate these quantities with the amount of preformed plasma in the cone.

The experiment was performed on the Titan laser at LLNL, of  $\lambda_0 = 1.054$   $\mu\text{m}$  wavelength,  $150 \pm 10$  J, focused to an 8  $\mu\text{m}$  full width at half maximum (FWHM) focal spot in a  $0.7 \pm 0.2$  ps pulse length. The intrinsic prepulse of the laser was measured at  $8 \pm 3$  mJ in a 1.7 ns duration pulse prior to the main beam. Varying prepulse levels, up to 1 J, were produced by injecting an auxiliary nanosecond-duration laser colinear with the main short pulse laser. This auxiliary laser had a similar focal spot distribution as the main beam and was timed to overlap the intrinsic prepulse.

The target, shown in Fig. 1, was a 1 mm long Au hollow cone with 30° full opening angle, 20  $\mu\text{m}$  wall thickness, 30  $\mu\text{m}$  internal tip diameter, and 11  $\mu\text{m}$  tip thickness. A 1.5 mm long, 40  $\mu\text{m}$  diameter Cu wire was glued to the outer cone tip. The wire diameter is chosen to match the nominal 40  $\mu\text{m}$  optimum ignition hot spot diameter in a FI target [7], and its quasi 1D geometry allows for single shot



- $K\alpha$  emission follows hot electrons in wire
- Find 2-temperature distribution required
- Laser-to-hot-electron efficiency measured

# New results on fast ignition

PRL 110, 025001 (2013)

PHYSICAL REVIEW LETTERS

week ending  
11 JANUARY 2013

## Effect of Target Material on Fast-Electron Transport and Resistive Collimation

S. Chawla,<sup>1,3</sup> M.S. Wei,<sup>2,\*</sup> R. Mishra,<sup>1</sup> K. U Akli,<sup>2</sup> C.D. Chen,<sup>3</sup> H.S. McLean,<sup>3</sup> A. Morace,<sup>1,4</sup> P.K. Patel,<sup>3</sup> H. Sawada,<sup>1</sup> Y. Sentoku,<sup>3</sup> R.B. Stephens,<sup>2</sup> and F.N. Beg<sup>1</sup>

<sup>1</sup>Center for Energy Research, University of California, San Diego, La Jolla, California 92093, USA

<sup>2</sup>General Atomics, P.O. Box 85608, San Diego, California 92186, USA

<sup>3</sup>Lawrence Livermore National Laboratory, Livermore, California 94551, USA

<sup>4</sup>Department of Physics, University of Milano Bicocca, Milano 20126, Italy

<sup>5</sup>Department of Physics, University of Nevada, Reno, Nevada 89557, USA

(Received 27 July 2012; published 7 January 2013)

The effect of target material on fast-electron transport is investigated using a high-intensity ( $0.7 \text{ ps}$ ,  $10^{20} \text{ W/cm}^2$ ) laser pulse irradiated on multilayered solid Al targets with embedded transport (Au, Mo, Al) and tracer (Cu) layers, backed with millimeter-thick carbon foils to minimize refluxing. We consistently observed a more collimated electron beam (36% average reduction in fast-electron induced Cu  $K\alpha$  spot size) using a high- or mid- $Z$  (Au or Mo) layer compared to Al. All targets showed a similar electron flux level in the central spot of the beam. Two-dimensional collisional particle-in-cell simulations showed formation of strong self-generated resistive magnetic fields in targets with a high- $Z$  transport layer that suppressed the fast-electron beam divergence; the consequent magnetic channels guided the fast electrons to a smaller spot, in good agreement with experiments. These findings indicate that fast-electron transport can be controlled by self-generated resistive magnetic fields and may have important implications to fast ignition.

DOI: 10.1103/PhysRevLett.110.025001

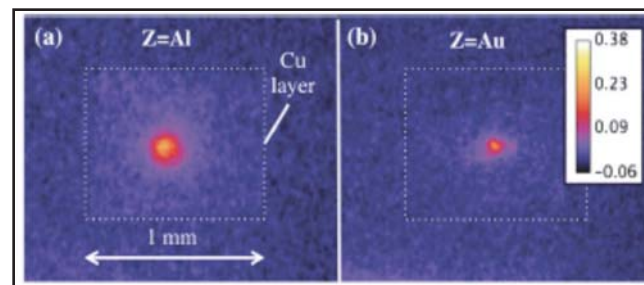
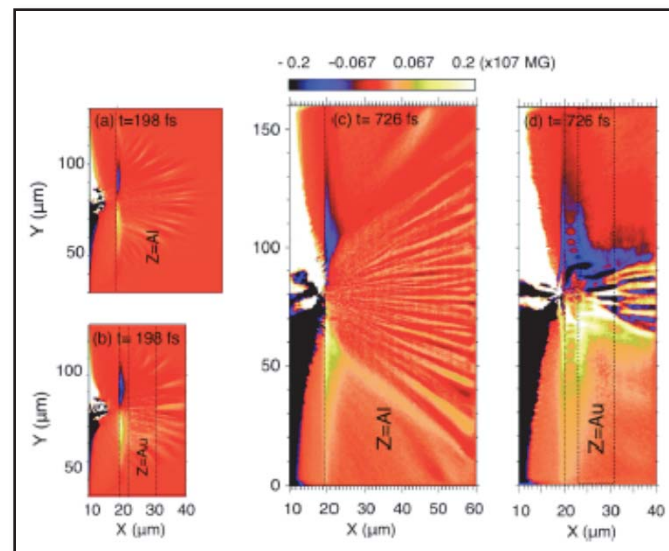
PACS numbers: 52.38.Dx, 52.38.Hb, 52.50.Jm, 52.65.Rr

Cone-guided fast-ignition (FI) inertial confinement requires efficient energy transport of high-intensity short-pulse-laser-produced relativistic (or “fast”) electrons through a solid cone tip to a high-density fuel core [1]. Specifically, successful ignition with a reasonably sized ignition laser requires high-conversion efficiency to 1–3 MeV electrons that have a minimum divergence [2,3]. Previous simulations show that fast-electron beam propagation in solid density plasmas are affected by a variety of mechanisms: scattering, resistive collimation [2,4], resistive filamentation [5], Ohmic heating, and electric field inhibition [6,7]. Evaluating the cone tip material, therefore, requires an understanding of the evolution of self-generated resistive fields and their cumulative effect on electron transport over the duration of the laser pulse. Previous material-dependent transport studies are limited; they have studied transport through only one material [8,9], simultaneously varied materials and fast-electron sources [10,11], or used energies much lower than presented here [11,12].

In this Letter, we report a systematic investigation of fast-electron transport in different materials (from high- $Z$  Au to low- $Z$  Al) without changing the electron source. We have demonstrated that a fast-electron beam can be collimated with a thin ( $\sim 10 \mu\text{m}$ ), high- or mid- $Z$  transport layer buried a few  $\mu\text{m}$  beneath a low- $Z$  Al layer without imposing a significant loss in forward-going electron energy flux. This is in contrast to previous 1D Fokker-Planck modeling predictions [13] that suggest high- $Z$  Au material would increase divergence due to scattering and reduce the

forward energy coupling, but it is consistent with the analytical model and 2D Fokker-Planck modeling showing stronger resistive collimation in high- $Z$  plasmas by Bell and Kingham [4]. In addition, the collimation did not rely on complex structured targets [14] or a double laser pulse configuration [15], as shown in recent experimental work.  $K\alpha$  fluorescence diagnostics, similar to those used in earlier work by Stephens *et al.* to measure fast-electron beam divergence [16], directly characterized fast-electron density distributions within the target. 2D collisional particle-in-cell (PIC) simulation results are in excellent agreement with experiments and show the formation, in high- $Z$  transport targets, of strong resistive magnetic channels enveloped by a global  $B$  field that collimate initially divergent fast electrons. These magnetic channels extend into the subsequent lower resistance layers, maintaining the guidance of fast electrons.

The experiment used the Titan laser ( $1 \mu\text{m}$  wavelength,  $150 \text{ J}$  in  $0.7 \text{ ps}$ ,  $17 \text{ mJ}$  average prepulse energy in  $2.3 \text{ ns}$ ) at the Jupiter Laser Facility, Lawrence Livermore National Laboratory. An  $f/3$  off-axis parabola focused the beam to a  $10 \mu\text{m}$  (FWHM) spot with an incident angle of  $17^\circ$  onto the target front surface at  $I_{\text{peak}} \sim 10^{20} \text{ W/cm}^2$ . Figure 1 shows a schematic of the multilayered solid target, laser beam, and x-ray diagnostics. Targets had a common Al front layer ( $3 \mu\text{m}$  thick), a  $Z$ -transport layer [Au ( $8 \mu\text{m}$ ), Mo ( $14 \mu\text{m}$ ), or Al ( $33 \mu\text{m}$ )], and a Cu tracer layer ( $22 \mu\text{m}$ ) buried  $110 \mu\text{m}$  behind the  $Z$ -transport layer. The common front Al layer for all targets was to provide an identical fast-electron source for the transport study.



- Different target materials affect hot  $e^-$  transport
- Self-generated magnetic fields can control hot electron divergence

0031-9007/13/110(2)/025001(5)

025001-1

© 2013 American Physical Society

# New results on relativistic laser-plasma interactions

PRL 109, 145006 (2012)

PHYSICAL REVIEW LETTERS

week ending  
5 OCTOBER 2012

## Dynamics of Relativistic Laser-Plasma Interaction on Solid Targets

Y. Ping,<sup>1</sup> A. J. Kemp,<sup>1</sup> L. Divol,<sup>1</sup> M. H. Key,<sup>1</sup> P. K. Patel,<sup>1</sup> K. U. Akli,<sup>2</sup> F. N. Beg,<sup>3</sup> S. Chawla,<sup>3</sup> C. D. Chen,<sup>1</sup> R. R. Freeman,<sup>4</sup> D. Hey,<sup>1</sup> D. P. Higginson,<sup>3</sup> L. C. Jarrott,<sup>3</sup> G. E. Kemp,<sup>4</sup> A. Link,<sup>4</sup> H. S. McLean,<sup>1</sup> H. Sawada,<sup>3</sup> R. B. Stephens,<sup>2</sup> D. Turnbull,<sup>5</sup> B. Westover,<sup>5</sup> and S. C. Wilks<sup>1</sup>

<sup>1</sup>Lawrence Livermore National Laboratory, Livermore, California 94550, USA

<sup>2</sup>General Atomics, San Diego, California 92186, USA

<sup>3</sup>Department of Mechanical and Aerospace Engineering, University of California-San Diego, La Jolla, California 92093, USA

<sup>4</sup>College of Mathematical and Physical Sciences, Ohio State University, Columbus, Ohio 43210, USA

<sup>5</sup>Department of Mechanical and Aerospace Engineering, Princeton University, Princeton, New Jersey 08544, USA

(Received 6 May 2011; published 5 October 2012)

A novel time-resolved diagnostic is used to record the critical surface motion during picosecond-scale relativistic laser interaction with a solid target. Single-shot measurements of the specular light show a redshift decreasing with time during the interaction, corresponding to a slowing-down of the hole boring process into overdense plasma. On-shot full characterization of the laser pulse enables simulations of the experiment without any free parameters. Two-dimensional particle-in-cell simulations yield redshifts that agree with the data, and support a simple explanation of the slowing-down of the critical surface based on momentum conservation between ions and reflected laser light.

DOI: 10.1103/PhysRevLett.109.145006

PACS numbers: 52.38-r, 52.27.Ny

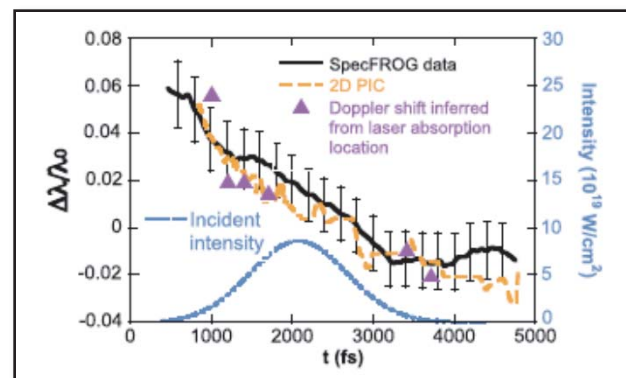
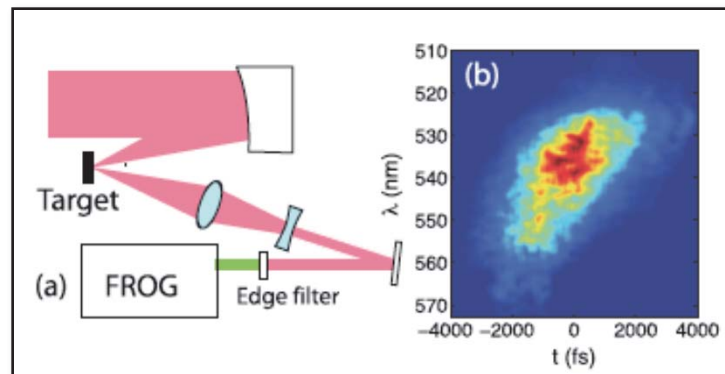
Relativistic laser-plasma interaction is of broad interest in modern physics, with applications ranging from particle acceleration [1], laboratory astrophysics [2], to fast ignition [3] for inertial confinement fusion [4]. During the interaction, the plasma conditions evolve rapidly upon intense laser irradiation, which modifies the partition of the deposited laser energy. Simulations have shown that the plasma density profile can be substantially steepened by the intense light pressure [5], which affects the energy spectrum of generated hot electrons [6] and their transport into the solid target [7]. Therefore time-resolved measurements are strongly desired to investigate the physical mechanisms and their consequences for various applications. However, among numerous studies of relativistic laser-plasma interaction, time-resolved measurements are quite scarce because the fast time scales (subpicosecond) and small spatial scales (micrometer) make these kinds of measurements very difficult.

Early time-resolved experiments on laser-plasma interaction at nonrelativistic intensities ( $\sim 10^{17}$  W/cm<sup>2</sup>) showed suppression of plasma expansion [8,9], and a transition from blue to red Doppler shift corresponding to the onset of hole boring [10]. Time-integrated data at  $10^{18}$  W/cm<sup>2</sup> [11] and  $10^{19}$  W/cm<sup>2</sup> [12] showed redshifts in the presence of preplasma, which can be explained by a simple model without taking into account the plasma thermal pressure [13]. In recent pump-probe experiments [14], Doppler spectrometry was used to study plasma motion up to 30 ps after the target was irradiated by a 30 fs laser at  $5 \times 10^{18}$  W/cm<sup>2</sup>. As intensities reach above  $10^{19}$  W/cm<sup>2</sup>, however, the process can change dramatically. Previous experiments have shown that the total absorption of laser pulses is strongly enhanced

in the relativistic regime [15]. As a result, the laser energy is deposited efficiently into the target, with substantial energy taken by energetic electrons. To study this effect on hole boring we have developed a novel time-resolved diagnostic based on frequency-resolved optical gating (FROG) [16] to measure the time history of the interaction in the relativistic regime [17]. Using this technique the frequency shift of specular light is measured in a single shot with a time resolution of  $\sim 100$  fs. We observed for the first time a continuously decreasing redshift that occurs even when the laser intensity is increasing. Particle-in-cell (PIC) simulations have been performed using measured laser parameters and the results agree well with the time-resolved data.

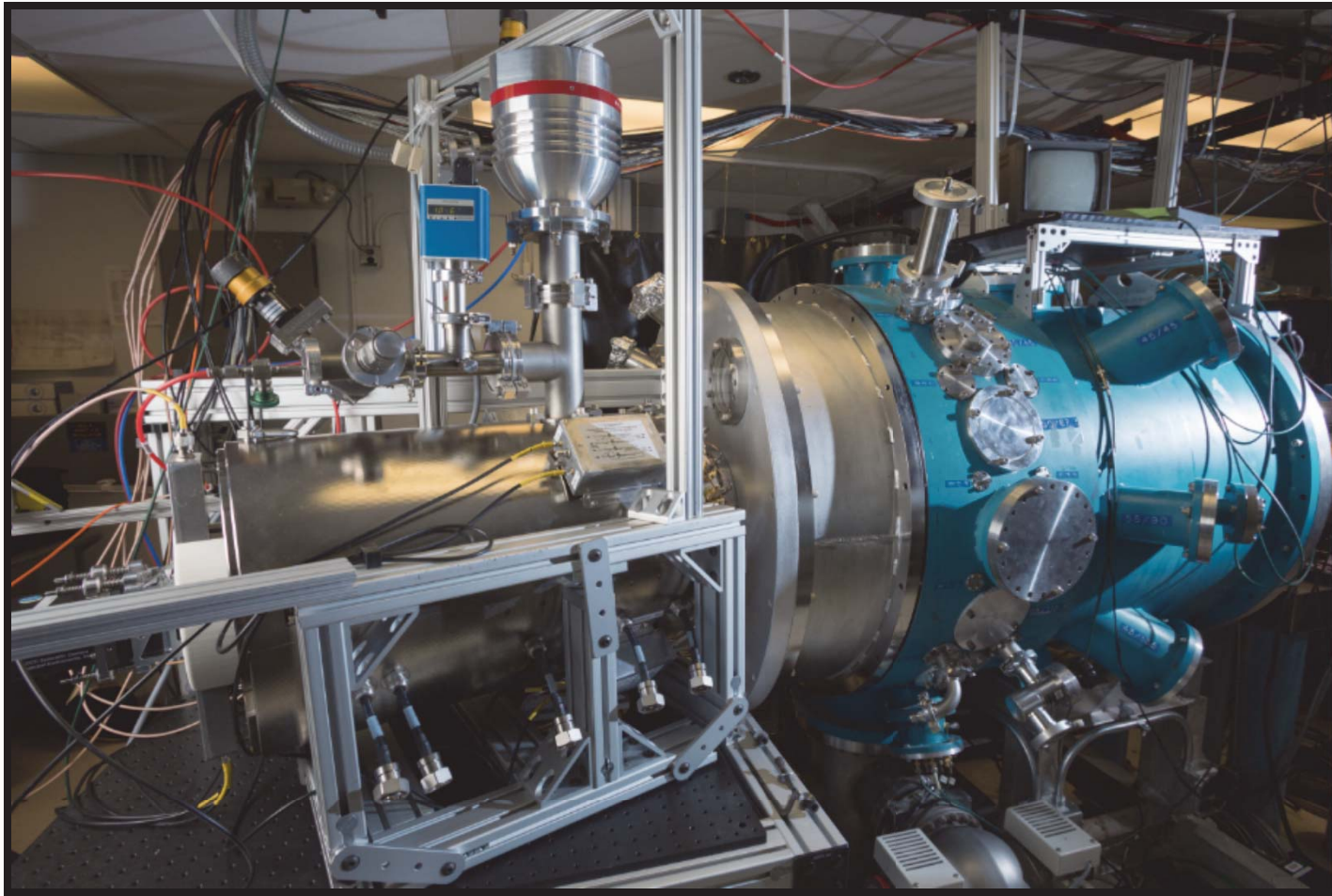
The experiment was performed on the Titan laser in the Jupiter laser facility at Lawrence Livermore National Laboratory. Titan is a Nd:glass laser system delivering 150 J, 1053 nm laser pulses as short as 0.7 ps at full width of half maximum (FWHM), or up to 300 J for 10 ps pulses. The experimental setup is illustrated in Fig. 1(a). The targets were simple 1 mm-thick slabs with aluminum as the front layer. The laser pulse was focused by an  $f/3$  off-axis parabola onto the target at an incident angle of  $10^\circ$ . The full characteristics of incident laser pulses were measured with a suite of on-shot laser diagnostics, including a FROG for the laser temporal shape and phase, a water cell for prepulses, and an equivalent plane monitor for the focal spot [18].

The light in the specular direction was collected by an  $f/10$  lens and collimated by a telescope before entering another FROG (specular FROG) operating near 527 nm with a polarization gating scheme [16]. An edge filter was inserted to reject the  $1\omega$  light. We chose  $2\omega$  because it was



- Developed FROG (Frequency-Resolved Optical Gating) for  $2\omega$
- Reveals critical surface motion with 100 fs resolution
- Evidence of decelerating plasma hole boring

# Recent highlights from Jupiter/COMET



# Highlights from COMET. COMET is used by NIF to calibrate and test diagnostics

## Studies of the mechanisms of powerful terahertz radiation from laser plasmas

Yutong Li\*, Guoqian Liao\*, Weimin Wang\*, Chun Li\*, Luning Su\*, Yi Zheng\*, Meng Liu\*,  
Wenchao Yan\*, Mulin Zhou\*, Fei Du\*, J. Dunn\*\*, J. Hunter\*\*, J. Nilsen\*\*, Zhengming Sheng\*\*\*,  
Jie Zhang\*\*\*

\* Beijing National Laboratory for Condensed Matter Physics, Institute of Physics, Chinese Academy of Sciences, Beijing 100190, China

\*\* Lawrence Livermore National Laboratory, 7000 East Avenue, Livermore, CA 94551, USA

\*\*\* Key Laboratory for Laser Plasmas (MoE) and Department of Physics, Shanghai Jiao Tong University, Shanghai 200240, China

Recently Terahertz (THz) radiation from laser-produced plasmas has attracted much interest since plasmas can work at arbitrarily high laser intensity. This paper will discuss the generation mechanisms of plasma-based THz radiation.

### I. INTRODUCTION

Terahertz radiation has been attracted much interest due to increasingly wide applications. Though THz radiation can be generated with various ways, it is still a big challenge to obtain strong tabletop sources. Plasmas, with an advantage of no damage limit, are promising medium to generate strong THz radiation [1]. THz radiation from femtosecond laser-induced plasma filaments in low density gases (particularly in air) has been reported. However, the radiation is found to be saturated with pump laser intensity. Recently THz radiation from intense laser-solid interactions has also been demonstrated. In principle, for solid targets the laser intensity can be arbitrarily high. The typical intensity of a multi-terawatt laser system is higher than  $10^{18}$  W/cm<sup>2</sup> (up to  $10^{21}$  W/cm<sup>2</sup> with a Petawatt laser). Using such ultraintense lasers, strong THz radiation with energies even up to mJ is expected. Intense laser-plasma interactions provide new opportunity to greatly enhance the THz source strength. On the other hand, the THz radiation can also be used as a new way to diagnose the interactions.

We have symmetrically studied strong THz radiation from solid targets driven by relativistic laser pulses. The experiments were carried out using femtosecond and picosecond laser systems, respectively. THz radiation with a pulse energy of tens  $\mu$ J/sr (driven by femtosecond laser), even  $\sim$ mJ/sr (driven by picosecond laser) is observed. In this talk, the THz polarization, temporal waveform, angular distribution and energy dependence on the laser energy will be presented. We find that the radiation is dependent on the preplasma density scale length. We believe that the THz radiation is probably attributed to the self-organized transient fast electron currents formed along the target surface for steep plasma density profile, while, the linear mode conversion mechanism when a large scale preplasma is presented.

### II. THz RADIATION FROM FEMTOSECOND LASER-SOLID INTERACTIONS FOR STEEP PLASMA PROFILE

Hamster *et al.* first demonstrated the generation of THz pulses with energies of  $1 \mu$ J/sr from solid aluminum targets irradiated by laser pulses at an intensity  $\sim 10^{19}$  W/cm<sup>2</sup> [2]. They believed that the THz radiation originated from the charge separation fields arisen from the longitudinal ponderomotive force at the critical density surface. THz pulses with  $0.5 \mu$ J/sr were also observed by Sagisaka *et al.* from Ti solid foil targets at a little bit lower laser intensity  $10^{17}$  W/cm<sup>2</sup> [3]. They proposed an "antenna" model to explain the observation, in which assumes that the electrons spread over the whole target and the target acts like an antenna. The spectrum of THz radiation from laser driven plasmas generated on a copper wire was measured using free-space electro-optic sampling by Gao *et al.* [4]. However, no clear evidence was found to show that the target size affects the THz radiation spectrum.

Our femtosecond experiments were carried out using the Xtreme Light II (XL-II) Ti: sapphire laser system at the Institute of Physics of the Chinese Academy of Sciences. A linearly-polarized laser pulse with an energy up to 150 mJ in 100 fs at 800 nm was focused onto a 30  $\mu$ m thick copper foil at an incidence angle  $67.5^\circ$  using an  $f/3.5$  off-axis parabolic mirror. A calibrated thermoelectric detector aligned in the laser specular direction was used to measure the THz pulse energy. Figure 1(a) shows the dependence of the THz pulse energy on pump laser energy. Each data point is taken by an average of  $\sim 10$  shots. The energy of the THz radiation monotonically increases with laser energy. For the laser energy of 130 mJ, the THz energy is up to  $5.5 \mu$ J in 0.11 sr. The temporal waveform was measured by a modified, single-shot electro-optic method with a chirped laser pulse, where a 1-mm thick ZnTe was used as the sampling crystal. It is found that the THz peak frequency is at about 0.5 THz. The frequency can be tuned by changing the laser incidence angle and plasma conditions.

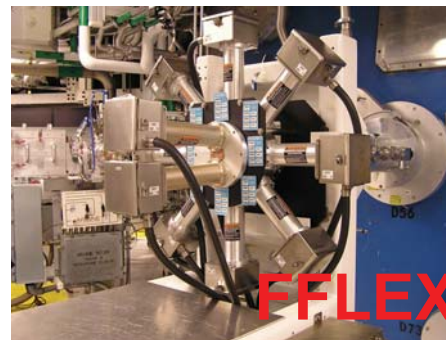
The strong THz radiation observed indicated that a net current should have been excited in the plasma. In the interaction of a relativistic laser pulse with a solid foil, due to the confinement of the spontaneous quasistatic magnetic and electrostatic fields at target surface, a lateral



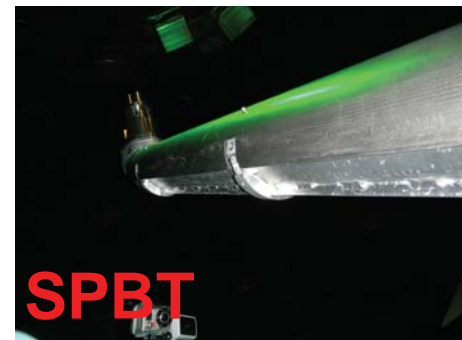
nTOF



DANTE



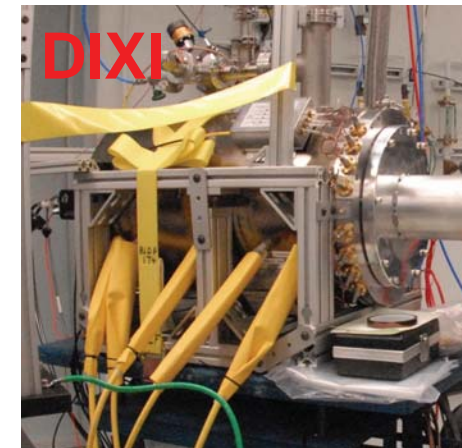
FFLEX



SPBT

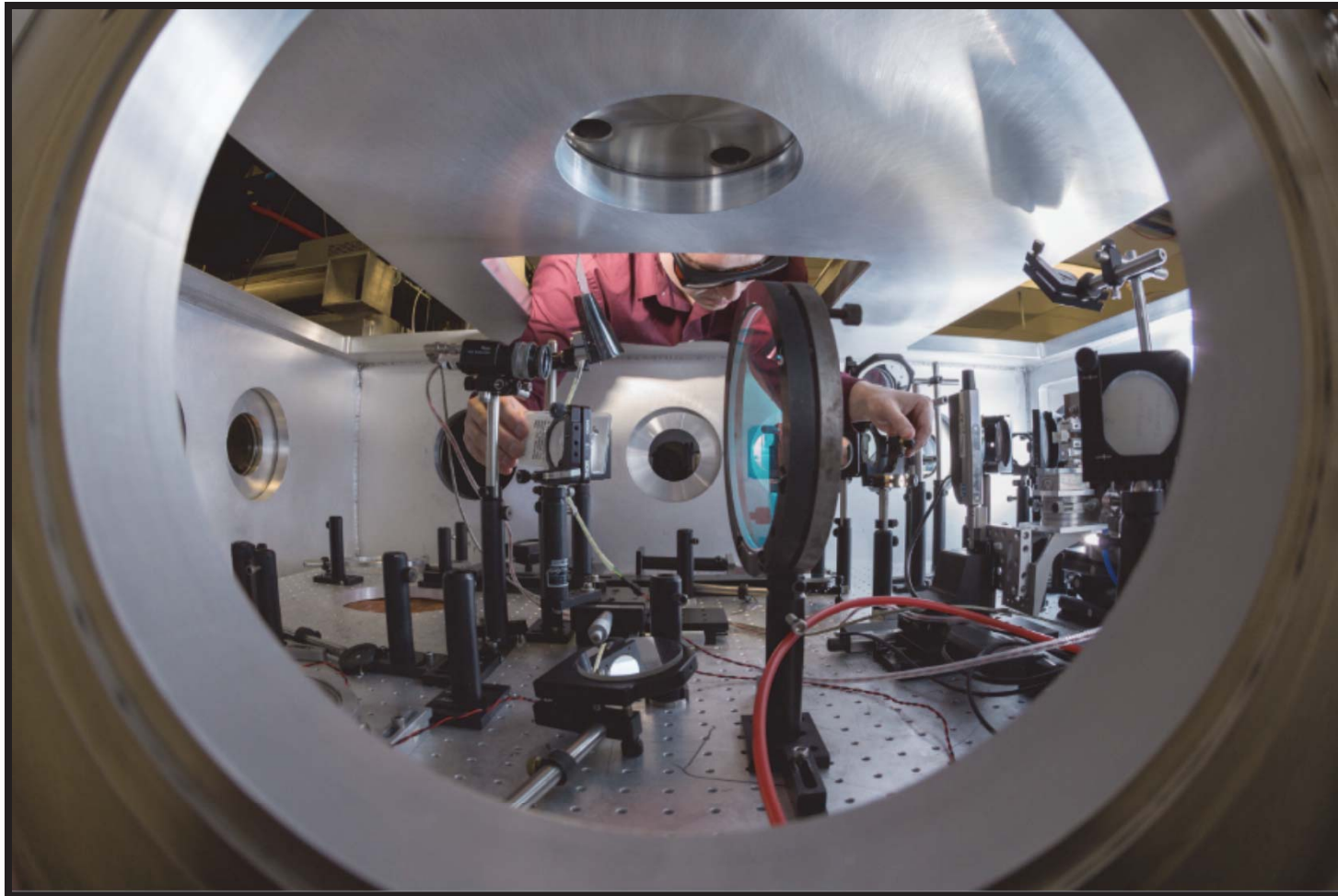


GXD



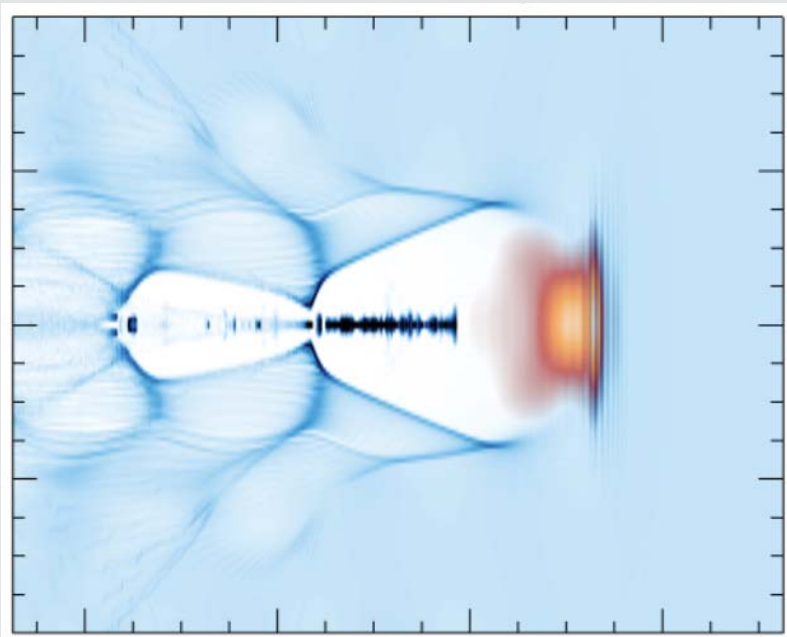
DIXI

# Recent highlights from Jupiter/Callisto



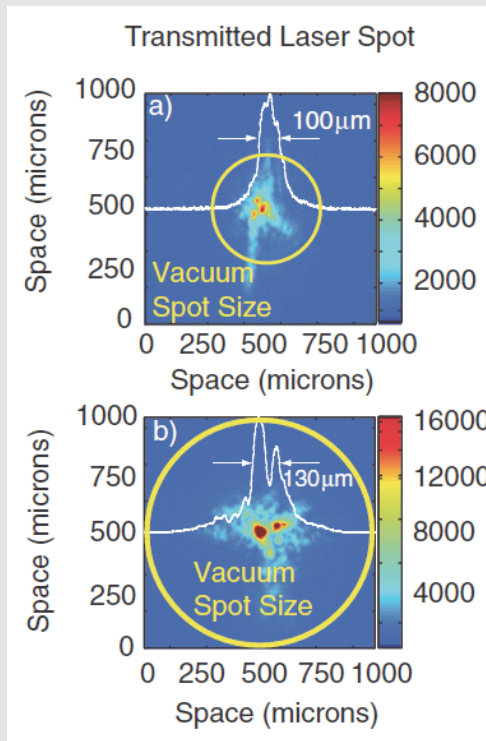
# LWFA measurements on Callisto show electron guiding and energy selection – talk by B Pollock

PIC simulations of this experiment predict electrons accelerated to GeV energies



Simulations show a bubble blown out by the beam. Injected electrons injected are accelerated

Self-guiding of wakefield-accelerated electrons results in small beam



Spectral measurements show the energy spread can be controlled to  $< 5\%$

# Jupiter is a multi-platform facility for high energy-density (HED) science

| Goal                                    | Metric   |   |
|---|--|---|
| Broad participation by LLNL researchers | Growth in LLNL user base   | Users up 200% in 4 years  |
| Expanded HED community                  | Growth in non-LLNL user base and expanding diversity of user institutions              | <ul style="list-style-type: none"> <li>- Users up 275% in 4 years</li> <li>- 56 universities</li> <li>- 20 institutes</li> </ul>      |
| Front-rank HED science                  | Publications   | <ul style="list-style-type: none"> <li>- ~24 journal publications/year</li> <li>- ~4 PRL/Science pubs/year</li> </ul>                 |
| Staging of expts to larger facilities   | Evidence of those expts at NIF, $\Omega$ , <i>etc.</i>                                 | XRTS, e <sup>+</sup> beams, ramp and Hugoniot EOS, FI, NLTE   |
| Development of novel HED diagnostics    | Implementation of diagnostics at NIF, $\Omega$ , <i>etc.</i>                           | 2D VISAR, p <sup>+</sup> radiography, fast detectors, x-ray sources   |
| Training of young researchers           | Growth in number of students, number of PhDs using JLF, and awards associated with JLF | <ul style="list-style-type: none"> <li>- 117 student users</li> <li>- 2 young researcher awards</li> <li>- 8 PhDs per year</li> </ul> |
| Pipeline into LLNL                      | Number of students hired by LLNL   | Since 2009, 14 of 32 PhDs hired at LLNL   |

# Number of active JLF users continues to increase

- **The number of JLF users is comparable to OMEGA**
- **However the budget has been flat, or less, for 5 years**
- **This has led to:**
  - **a reduction in number of shot weeks: 44 in 2008; 36 now**
  - **reduction in number of experiments: 38 in 2008; 29 now**
  - **and some frustration**

# Number of active JLF users continues to increase

- The number of JLF users is comparable to OMEGA
- However the budget has been flat, or less, for 5 years
- This has led to:
  - a reduction in number of shot weeks: 44 in 2008; 36 now
  - reduction in number of experiments: 38 in 2008; 29 now
  - and some frustration

**Demonstrates a need for intermediate-scale HED facilities,  
a need that is growing and continuing to grow**

# Status of Callisto

- Callisto was a very clever way of getting to 100 TW (10 J, 100 fs) in the last century
- A Janus long-pulse beam pumps an amplifier at the end of a very complex, custom (regen/bowtie on 3 optical tables) 200-mJ front end
- The pump is not monitored well and the pump energy varies by factor of 2
- The front end is variable in energy, astigmatic, and has a typically sub-par pre-pulse ( $10^{-4}$  contrast)
- Focus is usually good but pulse energies are hit-or-miss
- Cycle time limited by Janus pump laser (2/hr)
  
- Now used almost exclusively for LWFA; used by  $\sim 1/10$  number of users of other platforms
  
- Callisto could be made reliable at 400 TW with good contrast
  - cost would be about \$800K
  
- Good: maintains an ultra-short-pulse capability at LLNL; cheaper than diode-based system
  
- Bad: still limited by Janus rep rate; many high-rep-rate near-PW systems being built
  
- Funding request was disapproved. Callisto to be decommissioned this year.

# JLF discussion

- **JLF is funded almost entirely at the behest of LLNL S&T**
- **No indication that NNSA will help**
- **SC/FES is discussing a Bay Area HED Cooperative**
- **We have costed out several major improvements**

# Possible JLF upgrades



# JLF discussion

- **Stabilize JLF**
  - bring beams back to nominal energy
  - upgrade infrastructure
  - improved spare part inventory
  - system monitoring
  - more staff

-> *decreased downtime, better reproducibility, better reliability*
- **Improve JLF**
  - tailored pulseshapes (repeated requests)
  - increased beam energy (repeated requests)
  - available target area diagnostics (focal spot, energy, pulseshape)
  - prepulse monitoring
  - improved pulse contrast in Titan
  - 2<sup>nd</sup> short-pulse beam in Titan
- **Include OSL (Optical Science Laser)**
  - single beam, 1.5 kJ at  $1\omega$ ,  $3\omega$
  - different building, different organization

# Possible JLF upgrades – Titan pulse contrast

- **OPCPA contrast improvements (hybrid SPOPA approach)**

|   |                      |
|---|----------------------|
| – <b>Effort</b>   |                      |
| • Laser Scientist (0.75)                                  | \$167k               |
| • Machining & fabrication (0.5) technician                | \$120k               |
| • Diffraction grating processing (0.5)                    | \$ 70k               |
| – <b>Procurements: optics, electronics &amp; hardware</b> |                      |
| • Custom laser amplifiers                                 | \$ 90k               |
| • Grating substrates & processing                         | \$ 24k               |
| • OPA crystals  | \$ 20k               |
| • Misc hardware, optics, electronics                      | \$ 69k               |
| – <b>20% contingency</b>                                  | \$112k               |
| – <b>Total</b>  | <b><u>\$672k</u></b> |

- **Green short-pulse capability for Titan**

|  |                      |
|--|----------------------|
| – <b>Effort</b>  |                      |
| • Machining fabrication for mounts (3 man-weeks)         | \$ 13k               |
| • Design, assembly, alignment performed by JLF staff     | \$ 0                 |
| – <b>Procurements – mainly optics</b>                    |                      |
| • New full aperture (25cm CA) type I doubling crystal    | \$ 60k               |
| • New crystal mount hardware components                  | \$ 10k               |
| • $2\omega$ mirrors (5 each for 25cm beam)               | \$210k               |
| • High reflective/high damage threshold parabola coating | \$ 65k               |
| • Materials for fabrication                              | \$ 5k                |
| – <b>20% contingency</b>                                 | \$ 73k               |
| – <b>Total</b>   | <b><u>\$436k</u></b> |

# Possible JLF upgrades – second short-pulse Titan beam

- **2<sup>nd</sup> Titan short pulse beam upgrade**

- **Effort**

- Majority of effort supplied by JLF staff \$ 0k
- Fabrication by on-site services \$100k

- **Procurements**

- Optics \$532k
- Off-site machine procured services of existing designs \$230k
- Control & monitoring hardware & systems \$157k

- **20% contingency** \$204k

- **Total** **\$1223k**

*Fini*



# Comparison of LULI and JLF - capabilities

|                           | LULI                                       | JLF           |
|---------------------------|--|---------------|
| Shot Weeks per Year       | 30   | 36            |
| Long-pulse laser - Energy | 2 kJ                                       | 2 kJ          |
| LP Laser – Shots per Year | 600  | 600           |
| LP Laser – Expts per Year | 10   | 9             |
| Short-pulse Laser - Power | 100 TW                                     | 150 TW        |
| SP Laser - Shots per Year | 750  | 400           |
| SP Laser – Expts per Year | 10   | 3             |
| PW-Class Laser - Power    | Future 10 PW/0.1 Hz                        | 400 TW        |
| PW – Shots per Year       | N/A  | 500           |
| PW – Expts per Year       | N/A  | 9             |
| Moderate Energy Laser     | Future 20J/10 Hz                           | 12J/0.01 Hz   |
| Moderate – Expts per Year | N/A  | 8             |
| Funding                   | CNRS, CEA, EU                              | LLNL Overhead |
| Program                   | CNRS Center (10 Sci staff, 10 PDs, 20 GSs) | N/A           |

**LULI2000/Janus**

**ELFIE/Callisto**

**Apollon/Titan**

**Lucia/COMET**

# Comparison of LULI and JLF - staffing

|                                       | LULI  | JLF            |  |
|---------------------------------------|---|----------------|--|
| Laser Ops and Target Area Laser Techs | 14  | 6              | <b>Laser Operations/<br/>Experiments</b> |
| Target Area Expt Techs                | 6   | 0              |  |
| Laser System/Optics Support Techs     | 3   | 0              |  |
| Mechanical Techs                      | 5   | 3              | <b>Experiment Support</b>                |
| Instrumentation Techs                 | 4   | 0              |  |
| High Voltage Techs                    | 3   | 0              |  |
| Control/Interlock Techs               | 6   | 2              | <b>Facility Support</b>                  |
| IT Techs                              | 3   | 0              |  |
| Management/Admin                      | 3/9   | 1/1            |  |
| Other                                 | 23 techs on future projects (diode pump laser; 10 PW) | 0.5 Target Fab |  |

# Fini encore

## LLNL

Engineering  
NIF  
PLS  
WCI

Colorado St  
Columbia  
Florida A&M  
Harvard  
MIT  
Merchant Marine Acad  
Ohio State  
Princeton  
Rice  
Stanford  
Texas A&M  
U Arizona  
U Arkansas  
UC-Berkeley  
UC-Davis  
UCLA  
UC-Santa Barbara  
UC-San Diego  
U Colorado  
U Maryland  
U Michigan  
U Nevada Las Vegas  
U Nevada Reno  
U Rochester  
U Texas  
Vanderbilt  
Washington State  
West Point

Chinese Acad Science  
Ecole Polytechnique  
Gwangju IST  
Heinrich-Heine U  
Imperial College  
INRS - Montreal  
IST Lisbon  
Nat Inst Nucl Phys Italy  
Osaka U  
Queen's U Belfast  
Shanghai Jiao Tong U  
Tech U Darmstadt  
Tech U Dresden  
U Alberta  
U Bordeaux/CELIA  
U British Columbia  
U Edinburgh  
U Jena  
U Milano  
U Oxford  
U Paris  
U Pisa  
U Quebec  
U Rome  
U Strathclyde  
U Toronto  
U York  
Vienna U Tech

## Other

Alme/DTRA  
ARFL  
Carnegie Inst  
GA  
LANL  
LBNL  
LLE  
NRL  
NSTec  
NTF  
SLAC

AWE  
CEA  
CNR/Pisa  
DESY  
GSI  
JAEA Japan  
KAERI Korea  
Kentech  
RAL